

1969

Single crystal susceptibility study of one-dimensional antiferromagnetic interactions in CsCuC13

Frank Joseph Rioux III
Iowa State University

Follow this and additional works at: <https://lib.dr.iastate.edu/rtd>

 Part of the [Physical Chemistry Commons](#)

Recommended Citation

Rioux, Frank Joseph III, "Single crystal susceptibility study of one-dimensional antiferromagnetic interactions in CsCuC13 " (1969). *Retrospective Theses and Dissertations*. 4147.
<https://lib.dr.iastate.edu/rtd/4147>

This Dissertation is brought to you for free and open access by the Iowa State University Capstones, Theses and Dissertations at Iowa State University Digital Repository. It has been accepted for inclusion in Retrospective Theses and Dissertations by an authorized administrator of Iowa State University Digital Repository. For more information, please contact digirep@iastate.edu.

70-13,627

RIoux, III, Frank Joseph, 1942-
SINGLE CRYSTAL SUSCEPTIBILITY STUDY OF ONE-
DIMENSIONAL ANTIFERROMAGNETIC INTERACTIONS
IN CsCuCl_3 .

Iowa State University, Ph.D., 1969
Chemistry, physical

University Microfilms, Inc., Ann Arbor, Michigan

THIS DISSERTATION HAS BEEN MICROFILMED EXACTLY AS RECEIVED

SINGLE CRYSTAL SUSCEPTIBILITY STUDY OF ONE-DIMENSIONAL
ANTIFERROMAGNETIC INTERACTIONS IN CsCuCl_3

by

Frank Joseph Rioux, III

A Dissertation Submitted to the
Graduate Faculty in Partial Fulfillment of
The Requirements for the Degree of
DOCTOR OF PHILOSOPHY

Major Subject: Physical Chemistry

Approved:

Signature was redacted for privacy.

In Charge of Major Work

Signature was redacted for privacy.

Head of Major Department

Signature was redacted for privacy.

Dean of Graduate College

Iowa State University
Ames, Iowa

1969

TABLE OF CONTENTS

	Page
INTRODUCTION	1
LITERATURE SURVEY	3
One-Dimensional Systems	3
Theoretical	20
THEORY	26
EXPERIMENTAL	42
Single Crystal Data	51
DISCUSSION OF RESULTS	57
Bonding	57
Linear Antiferromagnetism	64
SUMMARY	76
BIBLIOGRAPHY	78
ACKNOWLEDGEMENTS	83
APPENDIX I	84
Ising Model	84
APPENDIX II	87
Bonner-Fisher Calculations	87
APPENDIX III	96
Molecular Orbitals for $\text{CuCl}_4^{=}$	96

LIST OF TABLES

	Page
Table 1. Calculated and observed crystal field splittings of CsCuCl_3 according to Day	4
Table 2. Magnetic properties of CuCl_2 , CuBr_2 and CrCl_2	12
Table 3. Eigenvalues and eigenfunctions for two electron system	32
Table 4. A-axis magnetic susceptibilities (exp. values)	52
Table 5. C-axis magnetic susceptibilities (exp. values)	53
Table 6. Results of least squares analyses	57
Table 7. Final atom position parameters for CsCuCl_3	61
Table 8. Atom positions for space group P_{6122}	61
Table 9. Perturbation matrix	89b
Table 10. Eigenvalues (in units of $E/ J $) and eigenvectors for $\gamma = 1.0$ for a ring of four spins	91
Table 11. Energies in units of $E/ J $ as a function of γ and S_z	92

LIST OF FIGURES

	Page
Fig. 1. Geometry of CuCl_4^{2-} complexes in CsCuCl_3	5
Fig. 2. The parallel susceptibility as a function of γ for a one-dimensional infinite chain spin $\frac{1}{2}$ antiferromagnet	40
Fig. 3. The perpendicular susceptibility as a function of γ for a one-dimensional infinite chain spin $\frac{1}{2}$ antiferromagnet	41
Fig. 4. Circuit diagram for Maxwell's mutual inductance bridge	43
Fig. 5. Circuit diagram for mutual inductance bridge	45
Fig. 6. Sample coils	46
Fig. 7. Cryostat system	48
Fig. 8. Sample support assembly	49
Fig. 9. Sample holders for the c- and z-axes	50
Fig. 10. χ_M as a function of temperature for the a- and c-axes	54
Fig. 11. χ_M^T as a function of temperature for the a- and c-axes	55
Fig. 12. $1/\chi_M$ as a function of temperature for the a- and c-axes	56
Fig. 13. Molecular orbital diagram for the square planar CuCl_4^{2-} complex	59
Fig. 14. Relative position of infinite chains in unit cell	66
Fig. 15. Comparison of theory and experiment for the parallel magnetic susceptibility. The	69

experimental parallel susceptibilities are the c-axis values

- Fig. 16. Comparison of theory and experiment for the perpendicular magnetic susceptibility. The experimental perpendicular susceptibilities are the a-axis values 70
- Fig. 17. Heat capacity as a function of temperature for powdered CsCuCl_3 71
- Fig. 18. Energy eigenvalues (in units of $E/|J|$) as a function of γ for a ring of four spins 93
- Fig. 19. Magnetic susceptibility as a function of reduced temperature for a ring of four spins for selected values of γ 95
- Fig. 20. Coordinate system for CuCl_4^- complexes 97

INTRODUCTION

One dimensionally interacting systems most simply test models of magnetic exchange and superexchange. Many one-dimensional systems (see literature review) are known, but few have simple bridging groups between metal ions, and are readily available in single crystal form. The double salt CsCuCl_3 is one of a series of ABX_3 systems being investigated in this laboratory for evidence of predominantly linear magnetic interactions in order to study the influence of translational symmetry upon a simple molecular orbital picture of what would appear, from the crystal structure, to be the predominantly interacting species in such compounds. This series was chosen for study because of the simplicity of the stoichiometry, the fact that the metal ions seem to form localized units (square planar CuCl_4^- units in CsCuCl_3 , planar Cu_2Cl_6^- dimer units in KCuCl_3 and LiCuCl_3 , octahedral NiCl_6^- chains in CsNiCl_3 and $(\text{CH}_3)_4\text{NNiCl}_3$) which might be amenable to a localized molecular orbital treatment to first order, which form chains all with a common halogen bridging groups, and because for the most part single crystals can be grown without unreasonable effort.

In our initial screening of some of these systems, powder susceptibility and heat capacity measurements were made in

order to determine if the systems exhibited behavior which might warrant further study. In particular, CsCuCl_3 (Rioux and Gerstein, 1969) was studied in such a manner, and it was found that, to a first approximation, the assumption of square planar CuCl_4^{\equiv} units being the predominant interacting species was not in conflict with the spectroscopic (Day, 1964) and magnetic behavior. In addition, it was found that while the powder susceptibility did not indicate three dimensional order, the heat capacity clearly exhibited behavior consistent with such ordering.

We felt it worthwhile to look more closely at the magnetic behavior via the single crystal magnetic susceptibility in order to determine the extent to which the assumption of isolated CuCl_4^{\equiv} could be extended, and because it appeared that single crystal behavior would provide a better understanding of the parameters involved in an anisotropic one-dimensional model of spin $\frac{1}{2}$ antiferromagnetically interacting units, as well as elucidate the nature of the ordering process in the neighborhood of 10°K .

LITERATURE SURVEY

Copper complexes exhibit a wide variety of magnetic properties, and because they are one of the simplest of magnetic systems, the literature on the magnetic properties of copper complexes is legion. Therefore this literature survey will consider only the literature on copper complexes exhibiting linear chain antiferromagnetism, which is the subject of this thesis. The literature survey will be divided into two parts; first, the experimental evidence for linear chain systems will be discussed, and then the theoretical developments in the field of linear antiferromagnetism will be reviewed.

One-Dimensional Systems

CsCuCl₃

Structural work (Wells, 1947a, Schleuter *et al.*, 1966) reveals that CsCuCl₃ consists of distorted hexagonally close-packed (CsCl₃) layers with the copper atoms in the octahedral holes. The octahedral holes are distorted in such a way that the copper's nearest neighbors are four chlorines in a plane, two chlorines at 2.355(4) Å and two chlorines at 2.281(6) Å. The next-nearest neighbors are two chlorines, one above and below the square plane, at 2.776(6) Å from the copper atom. The copper atoms are 0.42 Å from the 6-fold axis and are

oriented to form spiraling chains along the 6-fold axis. The copper-copper distance within the chains is $3.0621(10) \text{ \AA}$. This short distance is due to the fact that the copper atoms share faces of the chlorine octahedra. The structure is shown in Fig. 1.

Spectral work on CsCuCl_3 has been done by Day (1964). He determined the crystal field splittings by using a hexachlorobutadiene mull and by diffuse reflection. Using crystal field parameters evaluated from square planar Cu-Cl complexes, Day was able to calculate the observed transitions, and make an energy level assignment on the basis of his calculations. The level assignments, and comparison between calculated and experimental splittings are given in Table 1.

Table 1. Calculated and observed crystal field splittings of CsCuCl_3 according to Day (1964)

Assignment	Calc. (cm^{-1})	Obs. (cm^{-1})
$2B_{1g} \rightarrow 2E_g$	11,570	11,800
$2B_{1g} \rightarrow 2B_{2g}$	11,070	11,000

The magnetic susceptibility of CsCuCl_3 has been measured by Figgis and Harris (1959) in the temperature range $80\text{-}300^\circ\text{K}$. These authors found the effective magnetic moment to be 1.95

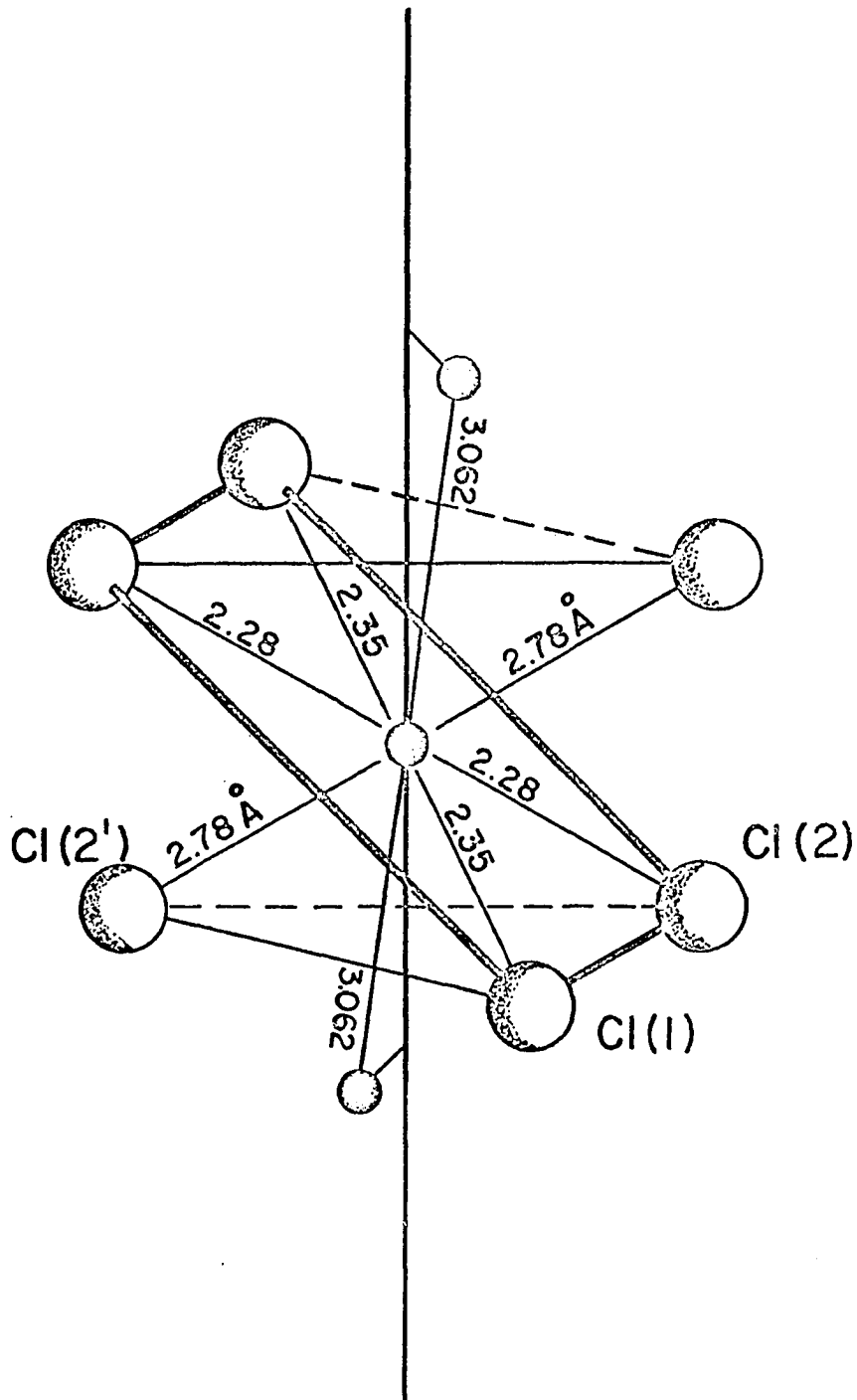


Fig. 1. Geometry of CuCl_4 complexes in CsCuCl_3

B.M. at 300°K and found the Weiss constant from a plot of $1/\chi$ vs T to be 1°K. On the basis of the crystal field diagram, the authors anticipated that CsCuCl_3 should obey Curie's law to low temperatures.

Recently, low temperature magnetic susceptibility (2 to 240°K) and heat capacity (5 to 300°K) measurements have been made on CsCuCl_3 powder (Rioux and Gerstein, 1969). It was found that the susceptibility deviated from Curie Law behavior at approximately 55°K. The susceptibility reached a maximum at 5°K and was essentially constant in the temperature range from 2° to 5°K. Calculations of g_{\parallel} and g_{\perp} based on a molecular orbital treatment of the square planar $\text{CuCl}_4^=$ complexes using the energy level assignments of Day (1964) were in agreement with the powder magnetic susceptibility.

The heat capacity measurements exhibited a λ -type anomaly at 10.4°K that strongly suggested that the system was ordering three dimensionally. However, no similar anomaly was observed in the magnetic susceptibility.

Recently, chlorine nuclear magnetic resonance studies have been performed (Rinneberg, Haas and Hartmann, 1969) on single crystals of CsCuCl_3 . These workers used the nmr technique to study the hyperfine interaction on the chlorine atoms

in the coordination sphere of the copper atoms. They compared their experimental evidence with molecular orbital calculations and found fair agreement. Their results will be discussed in greater detail later.

LiCuCl₃·2H₂O

The antiferromagnetic behavior of LiCuCl₃·2H₂O was reported first by Vossos, Jennings, and Rundle (1960). Magnetic susceptibility measurements by these workers on a powdered sample exhibited a maximum at 5.9°K (T_N), below which the magnetic susceptibility fell sharply. Above 5.9°K the susceptibility exhibits Curie-Weiss behavior, with a Weiss constant, $\theta = -10^{\circ}\text{K}$. The crystal structure of LiCuCl₃·2H₂O contains the nearly planar (Cu₂Cl₆)²⁻ dimers of approximately D_{2h} symmetry (Vossos, Fitzwater, and Rundle, 1963). The Cu-Cl distance in the dimer is about 2.3 Å, and the Cu-Cu distance is 3.399 Å. The dimers are connected to form chains through two Cu-Cl linkages of about 2.9 Å (Kato, Jonassen, and Fanning, 1964). Magnetic susceptibility data indicated that the salt was indeed dimeric and that the triplet state was probably the ground state, but that the predominant interaction between dimers forming one-dimensional infinite chains was antiferromagnetic. However, the neutron diffraction study accompanying the crys-

tal structure work of Abrahams and Williams indicates the spins on the copper ions are antiparallel and lie on the 3.47 Å Cu-Cu internuclear line (Abrahams and Williams, 1963).

Magnetic susceptibility measurements by these authors exhibited a peak at 6.5°K. Above 100°K, $1/\chi$ vs T was linear obeying Curie-Weiss law. The results of their investigation revealed that there are two predominant antiferromagnetic interactions in $\text{LiCuCl}_3 \cdot 2\text{H}_2\text{O}$. The first is between the Cu ions within each Cu_2Cl_6 dimer. The second is between copper ions on neighboring dimers along the a-axis with Cu-Cu distance of 3.84 Å. The next strongest interaction is ferromagnetic at a distance of 6.08 Å.

Heat capacity measurements on $\text{LiCuCl}_3 \cdot 2\text{H}_2\text{O}$ seem to indicate that the compound is not dimeric, since the magnetic entropy closely approximates $R \ln 2$ per mole of monomer rather than $R \ln 3$ per mole of dimer (Forstat and McNeely, 1961). NMR data confirm the antiferromagnetism of $\text{LiCuCl}_3 \cdot 2\text{H}_2\text{O}$, with $T_N = 4.46 \pm .02^\circ\text{K}$ (Spence and Murty, 1961). Spence and Murty believe the compound is dimeric and that the triplet is lower in energy than the singlet. They also suggest that the transition to the antiferromagnetic state corresponds to an ordering of the spin 1 dimers in the infinite chains.

KCuCl₃

A magnetic study on KCuCl₃ (Maass, Gerstein and Willett, 1967) indicates that the complex is dimeric and that the important species magnetically are the Cu₂Cl₆⁼ dimers. This is in agreement with structural data on KCuCl₃ (Willett, Dwiggin, Kruh and Rundle, 1963). The magnetic susceptibility data of Maass et al. was fit between 20 and 100°K assuming a singlet-triplet separation of 55°K. However, it does not now seem possible to exclude the possibility that the dimers are not independent. Thus it may be possible to explain the magnetic behavior of KCuCl₃ by postulating a strong spin-spin interaction within the dimers with the triplet state lying below the singlet, and then an antiferromagnetic interaction between the dimers on an infinite linear chain¹. The structural work of Willett et al. gives evidence of linear chains of dimers.

Cu(NH₃)₄SO₄·H₂O

Structural work (Mazzi, 1955) indicates that the Cu ions are located in linear chains parallel to the c-axis and are joined by a -Cu-H₂O-Cu-H₂O- linkage. The Cu-Cu distance

¹B. C. Gerstein, Dept. of Chemistry, Iowa State University, Ames, Iowa. 1969. Private communication to F. J. Rioux.

within the chain is 5.3 \AA . The linkage between coppers in neighboring chains is $-\text{Cu}-\text{NH}_3-\text{SO}_4-\text{NH}_3-\text{Cu}-$. Magnetic susceptibility data on powdered $\text{Cu}(\text{NH}_3)_4\text{SO}_4 \cdot \text{H}_2\text{O}$ exhibits a broad maximum at 3.5°K and a sharp peak at 0.37°K (Fritz and Pinch, 1957). Single crystal susceptibility measurements by Watanabe and Haseda (1958) indicate that the susceptibility is anisotropic and that the susceptibility along each of the crystallographic axes reaches a maximum at 3°K . Below 0.37°K the magnetic susceptibility along the C-axis is independent of temperature.

The heat capacity has been measured by Fritz and Pinch (1957) from 1.3 to 20°K and by Haseda and Miedema (1961) down to 0.03°K . Both research groups report a broad Schottky-type maximum in C_p near 3°K , and Haseda and Miedema have also observed a small sharp maximum at 0.37°K .

Griffiths (1964) has suggested that the anomalous susceptibility and heat capacity data can be explained by assuming strong antiferromagnetic interactions within the linear chains and at lower temperatures, around 0.37°K , three dimensional ordering of the copper ions on neighboring chains. He was able to show that both magnetic and thermal data could be fitted well using the calculations of Bonner and Fisher (1964) for linear chains of 10 and 11 spins coupled by an isotropic

Heisenberg interaction.

CuCl₂, CuBr₂, CrCl₂

Copper(II) chloride (Wells, 1947b), copper(II) bromide (Helmholz, 1947) and chromium(II) chloride (Handy, Gregory, 1951, and Cable, Wilkinson and Wollan, 1960) all have basically the same structure. The structure is composed of linear chains of $(\text{Cu,CrX}_2)_n$ formed by the sharing of edges of the squares of halides surrounding the metal ion. The packing of the chains is such that each metal ion has two more halide ions in its coordination sphere. These halide ions, one above and one below the copper ions, belong to neighboring $(\text{CuX}_2)_n$ chains. Thus, the site symmetry of each copper ion is distorted octahedral symmetry. The magnetic susceptibilities of CuCl₂ (DeHass and Gorter, 1931), CuBr₂ (Perakis, Serris and Karantassis, 1956) and CrCl₂ (Starr, Bitter and Kaufmann, 1940) have been measured to low temperatures. In all three compounds the magnetic susceptibility exhibits a broad maximum. In CuCl₂ the maximum occurs at 80°K, in CuBr₂ at 220°K and in CrCl₂ at 40°K. No single crystal magnetic susceptibility data are available for these complexes. Table II summarizes the powder magnetic susceptibility of these compounds.

Barracough and Ng (1964), with some success, have used a

Table 2. Magnetic properties of CuCl_2 , CuBr_2 and CrCl_2

Compound	Curie constant	Weiss constant	Temperature of max in X
CuCl_2	0.536	93°K	80°K
CuBr_2	0.450	246°K	220°K
CrCl_2	3.26	149°K	40°K

one-dimensional Ising model to explain the magnetic behavior of CuCl_2 and CuBr_2 . Stout and Chisholm (1962) have measured the heat capacity of CuCl_2 and CrCl_2 in the temperature range 11-300 $^\circ\text{K}$. These authors were able to evaluate the magnetic heat capacity and entropy of CuCl_2 and CrCl_2 by obtaining an approximation to the lattice heat capacity from the heat capacity of MnCl_2 . Sharp maxima occur in the heat capacities of CuCl_2 and CrCl_2 at $23.91 \pm 0.1^\circ\text{K}$ and $16.06 \pm .05^\circ\text{K}$, respectively. Both compounds also show a smaller, much broader maximum in their magnetic heat capacities at higher temperatures. (CuCl_2 around 40°K , CrCl_2 around 30°K). The results of their investigation support the belief that there is strong short-range magnetic order, arising from antiferromagnetic interactions between metal ions in a one-dimensional chain. At lower temperatures, three-dimensional, long-range order aris-

ing from interactions between neighboring chains becomes important. Stout and Chisholm were able to give an approximate theoretical explanation of the magnetic susceptibility, magnetic heat capacity and magnetic entropy using a one-dimensional Ising model to describe the weaker interchain interactions. The theoretical result for the magnetic susceptibility parallel to the chain direction is

$$\chi = \frac{Ng^2\beta^2 \exp(J/kT)}{4k[T + T_c \exp((J \pm J_c)/kT)]} \quad (1)$$

The term $T_c \exp((J \pm J_c)/kT)$ is due to the antiferromagnetic interaction between the neighboring chains.

CuCl₂ · 2H₂O

The crystal structure of copper(II) chloride dihydrate is similar to copper(II) chloride. The main difference being that Cl ions above and below the CuCl₄ square plane in CuCl₂ are replaced by waters of hydration (Poullis and Hardeman, 1952). The intrachain Cu-Cu distance is 3.73 Å. The Cu-Cu distance between chains is 5.5 Å. The magnetic properties are characterized by a Neel temperature, T_N of 4.33°K, but a broad maximum in the magnetic susceptibility at 4.8°K (Poullis and Hardeman, 1952). Marshall (1958) offered an explanation based upon the belief that in copper(II) chloride dihydrate the strongest

interaction between spins is within the linear $(\text{CuCl}_4^-)_n$ chains, and these interactions cannot support long-range order. Hence, the broad maximum in the magnetic susceptibility at 4.8°K . Long-range order is the result of next-nearest neighbor interactions of copper ions on neighboring chains. The ratio of the exchange interactions, J_2/J_1 is 0.138. J_1 is the strong short-range exchange constant and J_2 is the next-nearest neighbor exchange constant.

Rundle (1957) in analyzing N.M.R. data (Poullis and Hardeman, 1952) on $\text{CuCl}_2 \cdot 2\text{H}_2\text{O}$ was able to show that the unpaired magnetic electron is delocalized over the whole complex, spending 50% of its time on the Cu ion and 50% of its time on the chlorines. The large delocalization of the magnetic electron accounts for the success of the super-exchange mechanism operating in the linear chains. Rundle proposed that the three dimensional order was caused by interactions between antiferromagnetically ordered chains.

$\text{CuSO}_4 \cdot 5\text{H}_2\text{O}$

Structure determinations (Beavers and Lipson, 1934; and Bacon and Curry, 1962) on copper(II) sulphate pentahydrate indicate the presence of equal amounts of two different kinds of cupric ions. Heat capacity measurements by Geballe and

Giauque (1952) strongly support the conclusions drawn from the structural data. The heat capacity curve for a $\text{CuSO}_4 \cdot 5\text{H}_2\text{O}$ single crystal has a maximum at 1.35°K , a minor maximum at 0.75°K and a minimum at 0.25°K . At 0.25°K , $0.5R\ln 2$ of entropy has been lost, exactly half the magnetic entropy of a copper ion in $2s$ ground state.

Workers at the Kamerlingh Onnes Laboratory at Leiden (Miedema, van Kempen, Haseda and Huiskamp, 1962) have performed low temperature heat capacity and magnetic susceptibility measurements on copper(II) sulphate pentahydrate. Their measurements are in the temperature region 0.03 to 1°K . They observed a maximum in the heat capacity near 1°K . No maximum was observed at 0.75°K . The heat capacity rises again after 0.25°K . These workers also found that $0.5R\ln 2$ e.u. are lost above 0.25°K , strengthening the belief that there are essentially two independent magnetic systems of copper ions in $\text{CuSO}_4 \cdot 5\text{H}_2\text{O}$.

It is postulated that one of the systems consists of infinite chains of cupric ions which are coupled by an isotropic Heisenberg $\hat{S}_i \cdot \hat{S}_{i+1}$ interaction. The other system of cupric ions is paramagnetic at temperatures above 0.25°K . The magnetic susceptibility measurements of the Leiden group bear this idea out. After the paramagnetic term from system II is

subtracted from the total susceptibility, the remainder can be explained by considering the system a one-dimensional Heisenberg antiferromagnet.

More recently, N.M.R. (Wittekoek, Poulis and Miedema, 1964) and refined heat capacity (Anderson and Giaque, 1962) measurements have been performed on $\text{CuSO}_4 \cdot 5\text{H}_2\text{O}$. Both of these investigations show further support for the model proposing two independent magnetic systems of cupric ions. $\text{CuSeO}_4 \cdot 5\text{H}_2\text{O}$ exhibits the same behavior magnetically as $\text{CuSO}_4 \cdot 5\text{H}_2\text{O}$.

$\text{Cu}(\text{NH}_3)_4(\text{NO}_3)_2$

Electron spin resonance data has indicated a strong exchange interaction in $\text{Cu}(\text{NH}_3)_4(\text{NO}_3)_2$ (Okamura and Date, 1954). Rogers and Dempsey (1961) have measured the heat capacity from 1.2 to 16°K. The results show a broad maximum similar to those reported in substances with linear chains of magnetic ions. Comparison of the heat capacity results with the theory of Bonner and Fisher (1964) has led these workers to propose that $\text{Cu}(\text{NH}_3)_4(\text{NO}_3)_2$ contains isolated linear chains of Cu ions and the nearest-neighbor Heisenberg interaction constant is $J/k = 3.7 \pm .04^\circ\text{K}$. However, preliminary crystal structure studies do not indicate the presence of linear chains.

Dichloro(1,2,4,-triazole)copper(II) and copper(II) benzoate trihydrate

The magnetic susceptibilities of dichloro(1,2,4,-triazole)copper(II) and copper(II) benzoate trihydrate have been measured in the temperature range of 4.2° to 300°K (Inoue, Emori and Kubo, 1968). The susceptibilities of both complexes can be considered to be a sum of two terms. One term is a low temperature paramagnetic contribution, the other term is that of a linear chain antiferromagnet. Because of the purity of the samples the authors have ruled out impurities as the cause of the paramagnetic contribution. After subtracting the paramagnetic contribution the magnetic susceptibility does indeed have all the characteristics of a one-dimensional linear chain antiferromagnet. J/k for dichloro(1,2,4,-triazole)copper(II) is -17.9°K and for copper(II) benzoate trihydrate it is -12.7°K . The crystal structures of these complexes definitely indicate the presence of linear chains. The site symmetry of dichloro(1,2,4,-triazole)copper(II) (Jarvis, 1962) is distorted octahedral, the coordination sphere being made up of a plane of four chlorine atoms, with two nitrogens on the tetragonal axis. The chains are formed by the sharing of edges of the octahedrons and by linkage through the 1,2,4-triazole molecules.

The Cu-Cu distance is 3.40 Å.

Copper(II) benzoate trihydrate (Koizumi et al., 1963) has a similar structure. The neighboring coppers in the chain are 3.15 Å apart and they are bridged by two oxygen atoms on the edge of the octahedron and by a Cu-O-C-O-Cu linkage.

Miscellaneous

The structure of KCuBr₃ (Willett et al., 1963) indicates the presence of dimers. The magnetic susceptibility exhibits a broad maximum at 129°K, indicative of the behavior of binuclear copper(II) acetate. However, the susceptibility data cannot be fitted successfully in terms of an equilibrium between singlet and triplet spin states (Inoue, Kishita and Kubo, 1967). The magnetic susceptibility of a complex with a singlet ground state and low lying excited triplet state is

$$\chi = \frac{Ng^2\beta^2}{3kT} [1 + 1/3 \exp(J/kT)]^{-1} + N\alpha. \quad (2)$$

In order to explain their susceptibility data Inoue et al. have proposed that the magnetic moment of each dimer is subjected to a Weiss field caused by the other dimers. This is accounted for theoretically by the θ in the following expression,

$$\chi = \frac{Ng^2\beta^2}{3k(T+\theta)} [1 + 1/3 \exp(J/kT)]^{-1} + N\alpha. \quad (3)$$

A good fit is obtained with this formula over the whole temperature range when the parameters have the following values; $g = 2.00$, $J/k = 195^\circ\text{K}$, $\theta = -17^\circ\text{K}$ and $N\alpha = 60 \times 10^{-6}$.

The magnetic properties of copper(II) oxalate can be explained assuming one-dimensional linear chains of copper ions (Dubicki, Harris, Kokot and Martin, 1966). The susceptibility shows a broad maximum at 260°K . The experimental data cannot be fitted assuming singlet-triplet equilibrium of a binuclear complex. Structural work does not seem to exist, so Dubicki et al. have proposed a structure.

It appears that copper(II) succinate, copper(II) glutarate and copper(II) suberate have a predominant spin-spin interaction within the dimers and a linear antiferromagnetic interaction between the dimers within infinite chains (Figgis and Martin, 1966). This is similar to the interactions proposed for KCuBr_3 .

$\text{Cu}_3\text{Cl}_6(\text{C}_6\text{H}_7\text{NO})_2 \cdot 2\text{H}_2\text{O}$ has an interesting crystal structure (Sager and Watson, 1968). The structure consists of $\text{Cu}_2\text{Cl}_4 \cdot (\text{C}_6\text{H}_7\text{NO})_2$ dimers bridged together into infinite chains by $\text{CuCl}_2 \cdot 2\text{H}_2\text{O}$ groups. This again is roughly similar to the case of KCuBr_3 . In this complex, however, the bridging groups between magnetic dimers are themselves magnetic groups. Mag-

netic susceptibility data is only available down to 77°K (Kidd et al., 1967). The magnetic moment is only slightly temperature dependent in the temperature range 77 to 300°K. Clearly low temperature magnetic susceptibility data is needed to elucidate the nature of the magnetic interactions in this complex. It will be particularly interesting to see how the $\text{CuCl}_2 \cdot 2\text{H}_2\text{O}$ groups behave when complexed with the larger $\text{Cu}_2\text{Cl}_4 \cdot (\text{C}_6\text{H}_7\text{NO})_2$ groups.

The spectral and magnetic properties of copper(II) cyanoacetate (Wasson, Skyr and Trapp, 1968) indicate that the structure is basically dimeric with polymerization of the dimers via the nitrogen end of the cyano groups. The magnetic properties of copper(II) methoxide can be fitted by a linear chain one-dimensional Ising model (Adams, Barraclough, Martin and Winter, 1967). No structural data is yet available.

Theoretical

Theoretical interest in one-dimensional magnetic systems has increased markedly in the last ten years. Evidently this is due to the discovery of a large number of systems (see previous section) which magnetically, at least, are one-dimensional. The problem of a linear chain of spin $\frac{1}{2}$ atoms is a statistical mechanical problem which was first attacked by

Ising in 1925. He sought to explain ferromagnetism as the result of interactions between the spins on adjacent atoms. He assumed for simplicity an interaction of the form,

$$H = -2J \sum_{i=1}^N \hat{S}_i^z \cdot \hat{S}_{i+1}^z \quad (4)$$

whose energy eigenvalues and thus thermal and magnetic properties can be obtained exactly for a one-dimensional infinite chain.

Since it can be shown that a one-dimensional chain of spin $\frac{1}{2}$ atoms cannot exhibit cooperative phenomenon, Ising and the rest of the scientific community lost interest in this approach as a comprehensive theory of magnetism. It was not until the middle of the 1950's, when many one-dimensional systems were discovered, that interest in the Ising model was renewed. The Ising model has been the subject of three major review articles; two discuss the statistical mechanics of the model (Newell and Montroll, 1953; and Domb, 1960) and the other is of a historical nature (Brush, 1967).

One of the objections to the Ising model of antiferromagnetism is that for certain critical magnetic fields it predicts a non-zero entropy which persists down to 0°K (Brooks and Domb, 1951; Domb, 1960; Fisher, 1960) in violation of the

Third Law of Thermodynamics. Fisher (1960) proposed that this problem was peculiar to the Ising model and due to the simplicity of the Ising coupling interaction. Fisher suggested that the non-zero entropy at 0°K would not be observed with more realistic forms of the interaction Hamiltonian. Bonner and Fisher (1962) have shown that the problem of non-zero entropy at 0°K vanishes if the anisotropic Heisenberg Hamiltonian,

$$\mathcal{H} = -2J \sum_{i=1}^N (\hat{S}_i^z \cdot \hat{S}_{i+1}^z + \gamma(\hat{S}_i^x \cdot \hat{S}_{i+1}^x + \hat{S}_i^y \cdot \hat{S}_{i+1}^y)), \quad (5)$$

is used to represent the coupling between nearest neighbor spins. Although the completely anisotropic interaction proposed by Ising is not considered to be physically realistic, there is no question of the great importance of his work.

Stout and Chisholm (1962) developed a theory of linear chain antiferromagnetism which is essentially an Ising model with a molecular field. This model is attractive because it qualitatively explains the magnetic behavior of many one-dimensional systems and provides an approximate quantitative explanation of the heat capacity and magnetic susceptibility of CrCl_2 and CuCl_2 , two linear chain antiferromagnets. Basically the Ising model accounts for the strong short-range

ordering effects which produce broad maxima in the magnetic heat capacity and magnetic susceptibility, and the molecular field accounts for the weaker three-dimensional interactions between different chains which produce λ -type anomalies in both the heat capacity and magnetic susceptibility. Calculations of the magnetic heat capacity based on the model of Stout and Chisholm show a sharp peak at low temperatures and a lower, broader maximum at high temperatures. The major short-coming of this model would seem to be its reliance on the completely anisotropic coupling of the Ising model.

Orbach (1959) calculated the eigenvalues of the isotropic Heisenberg Hamiltonian

$$\mathcal{H} = 2J \sum_{i=1}^N (\hat{S}_i \cdot \hat{S}_{i+1} - \frac{1}{2}) \quad (6)$$

for rings of 2, 4, 6, 8 and 10 spin $\frac{1}{2}$ atoms. Griffiths (1961) calculated the energy, entropy, specific heat and magnetic susceptibility for rings of spin $\frac{1}{2}$ atoms containing 2,3,...10 atoms. The calculations were carried out using the isotropic ($\gamma = 1$) Heisenberg Hamiltonian to describe the interactions between spins. Griffiths was able to show that the convergence in the calculation of the thermal and magnetic properties as the ring size increased was rapid and that the thermodynamic and magnetic quantities for rings of 9 and 10 spins provide a

good approximation to the infinite chains above temperatures of $|J|/k$. Here, J is the exchange integral and k is Boltzmann's constant.

The most comprehensive treatment of the thermodynamic and magnetic properties of linear chain systems is given by Bonner and Fisher (1964). (See Appendix II). Their work differs from Griffith's in that they use an anisotropic Heisenberg Hamiltonian ($\gamma = 0$ to 1.0) for the coupling between nearest neighbor spins. They made the calculation for 2 through 11 spins for both ferro- and antiferro-magnetic coupling. Bonner and Fisher estimated thermal and magnetic properties for $T < |J|/k$ by extrapolation. Since they also determined the eigenfunctions of the anisotropic Hamiltonian they were able to calculate short-range and long-range order. The treatment of Bonner and Fisher of the magnetic properties for linear chains is the one which will be used in this work.

Zoltan G. Soos (1965, 1966) has applied a pseudospin approach to linear antiferromagnetism in organic crystals. The Hamiltonian employed to express the coupling between nearest neighbor spins is an alternating Heisenberg Hamiltonian,

$$H = \sum_{i=1}^{N/2} (J(1+\delta)\hat{S}_{2j} \cdot \hat{S}_{2j-1} + J(1-\delta)\hat{S}_{2j} \cdot \hat{S}_{2j-1} - \frac{1}{2}J). \quad (7)$$

The procedure in applying this Hamiltonian to one-dimensional systems is to transform the Hamiltonian first to Fermi creation and annihilation operators and then to pseudospin operators. The parameter, δ , is varied from 0 to 1.

Duffy and Barr (1968) have calculated the energy, entropy, specific heat and magnetic susceptibility for chains of 4, 6, 8, 10 spin $\frac{1}{2}$ atoms, using the alternating Heisenberg Hamiltonian,

$$\mathcal{H} = 2J \sum_{i=1}^{N/2} (\hat{S}_{2i} \cdot \hat{S}_{2i-1} + a \hat{S}_{2i} \cdot \hat{S}_{2i+1}). \quad (8)$$

They also show that behavior for infinite chains is well approximated by chains of 10 atoms. This approach and the approach of Soos seems to be well-suited to organic free radicals.

THEORY

A large number of substances have zero-field magnetic susceptibilities with a $1/T$ temperature dependence.

$$\chi = \frac{C}{T} + \alpha \quad (9)$$

The nature of this temperature dependence was first realized by Curie in 1895. A paramagnet with magnetic susceptibility exhibiting a temperature dependence of this form is said to obey Curie's Law.

A quantum mechanical derivation of Curie's Law is not difficult to give. To determine the effect of the magnetic field on the energy levels of a paramagnetic ion we write both the Hamiltonian and the energy of a particular state in a power series in H , the magnetic field,

$$\mathcal{H} = \mathcal{H}_0 + H\mathcal{H}_1 + H^2\mathcal{H}_2 + \dots \quad (10)$$

and

$$E_n = E_n^0 + HE_{n,m}^{(1)} + H^2E_{n,m}^{(2)} + \dots \quad (11)$$

Here \mathcal{H}_0 is the Hamiltonian for the system in the absence of a magnetic field and E_n^0 is the energy of the n th state in the absence of a magnetic field. The m arises because the n th energy level may be degenerate in the absence of the magnetic field and this degeneracy may be removed by the magnetic field.

From perturbation theory (Van Vleck, 1932) it is known that

$$E_{n,m}^{(1)} = \langle \psi_{n,m} | \mathcal{H}_1 | \psi_{n,m} \rangle, \quad (12)$$

and

$$E_{n,m}^{(2)} = \sum_{n',m'} \frac{|\langle \psi_{n',m'} | \mathcal{H}_1 | \psi_{n,m} \rangle|^2}{E_{n,m} - E_{n',m'}} + \langle \psi_{n,m} | \mathcal{H}_2 | \psi_{n,m} \rangle, \quad (13)$$

where

$$\mathcal{H}_1 = -g\beta \sum_i (\hat{L}_i + \hat{S}_i) \quad (14)$$

and

$$\mathcal{H}_2 = \sum_i (e_i^2 / 8m_i c^2) (\hat{x}_i^2 + \hat{y}_i^2). \quad (15)$$

$E_{n,m}^{(1)}$ is called the first order Zeeman correction to the n th energy level and, as we shall see, determines the Curie constant. $E_{n,m}^{(2)}$ is the second-order Zeemann correction to the n th level and is the temperature independent term in Equation 9.

An expression for the magnetic moment can be obtained from Equation 11 (Van Vleck, 1932)

$$\mu_{n,m} = - \frac{\partial E_n}{\partial H} = -E_{n,m}^{(1)} - H E_{n,m}^{(2)}. \quad (16)$$

If it is now assumed that the magnetic ions of a paramagnetic salt are independent of one another we may calculate the net magnetic moment of a mole of such a salt using a simple Boltzmann distribution.

$$\langle M \rangle = \frac{N \sum_{n,m} \mu_{n,m} \exp(-E_n/kT)}{\sum_{n,m} \exp(-E_n/kT)} \quad (17)$$

We now expand the exponential terms

$$\exp(-E_n/kT) \cong \exp(-E_n^0/kT) (1 - HE_{n,m}^{(1)}/kT) . \quad (18)$$

Clearly this type of expansion is only good when $(HE_{n,m}^{(1)})/kT$ is small compared to unity. This is why the susceptibility calculated in this manner is called the zero field magnetic susceptibility. Thus using Equations 16, 17 and 18

$$\langle M \rangle = \frac{N \sum_{n,m} (-E_{n,m}^{(1)} - 2HE_{n,m}^{(2)}) (1 - HE_{n,m}^{(1)}/kT) \exp(-E_n^0/kT)}{\sum_n \exp(-E_n^0/kT)} . \quad (19)$$

Notice that in the partition function even the $HE_{n,m}^{(1)}/kT$ term is neglected, stressing further that this calculation is valid only in the limit of zero magnetic field. Rearranging Equation 19 we can now write

$$\langle M \rangle = \frac{N \sum_{n,m} [H(E_{n,m}^{(1)})^2/kT - 2HE_{n,m}^{(2)} - E_{n,m}^{(1)} - H^2 E_{n,m}^{(1)} E_{n,m}^{(2)}] \exp(-E_n^0/kT)}{\sum_{n,m} \exp(-E_n^0/kT)} \quad (20)$$

In the absence of a magnetic field a paramagnetic substance has no net magnetic moment so the sum,

$$\sum_{n,m} E_{n,m}^{(1)} \exp(-E_n^0/kT) , \quad (21)$$

is zero. Approximating further by keeping only first order terms in the magnetic field, H , we write

$$\langle M \rangle = \frac{N \sum_{n,m} [H(E_{n,m}^{(1)})^2/kT - 2HE_{n,m}^{(2)}] \exp(-E_n^0/kT)}{\sum_n \exp(-E_n^0/kT)} \quad (22)$$

Thus the magnetic susceptibility for a mole of magnetically independent ions is

$$\chi = \frac{\langle M \rangle}{H} = \frac{N \sum_{n,m} [(E_{n,m}^{(1)})^2/kT - 2E_{n,m}^{(2)}] \exp(-E_n^0/kT)}{\sum_n \exp(-E_n^0/kT)} \quad (23)$$

It is important to stress the approximations which were made in the derivation of Equation 23. In writing Equation 17 it is assumed that the magnetic moments of the individual ions are independent which is only true in the temperature range in which dipole-dipole and exchange effects are small compared to kT . In the developments from Equation 17 to 23 repeated approximations were made which were based on the assumption that βH is small compared to kT . In this work an a.c. mutual inductance bridge was used to measure the magnetic susceptibility. The fields employed in this technique are on the order of 10 gauss, which means that for all practical purposes we measure zero field magnetic susceptibilities.

Many paramagnets do not maintain their paramagnetism over wide temperature range. The deviations occur at tempera-

tures high enough that they cannot be attributed simply to dipole-dipole interactions. Weiss (Smart, 1966) proposed that deviations from paramagnetism were due to a molecular field and the effect of this field on the magnetic susceptibility of a paramagnet above the ordering temperature is taken into account by the parameter θ in the following expression

$$\chi = \frac{C}{T+\theta} + \alpha . \quad (24)$$

If θ is negative the transition is to a ferromagnetic state, if it is positive the transition is to an antiferromagnetic state. Antiferromagnetism was not known until 1932 (Neel, 1932).

A feeling for the molecular field can be had by assuming that its origin lies in an exchange coupling between spins of the form

$$\mathcal{H} = -2J\hat{S}_1 \cdot \hat{S}_2 , \quad (25)$$

where J is the exchange integral and \hat{S}_1 and \hat{S}_2 are the total spin operators for spins 1 and 2. We will investigate the effect of the perturbation on the energy levels of a two spin system.

Since there are two spins there are 2^2 or 4 wavefunctions for our system, because each spin can have S_z values of $\pm \frac{1}{2}$. Thus the possible wavefunctions for this system are

$$\begin{aligned}
\psi_1 &= 1|++\rangle, \\
\psi_2 &= 1|+-\rangle, \\
\psi_3 &= 1|-+\rangle, \\
\psi_4 &= 1|--\rangle.
\end{aligned}
\tag{26}$$

The + and - refer to $S_z = +\frac{1}{2}$ and $S_z = -\frac{1}{2}$, respectively. Because we have chosen to write our wavefunctions in terms of the S_z values of the individual spins we will have to write our Hamiltonian in terms of operators which are convenient,

$$\mathcal{H} = -2J(\hat{S}_1^z \cdot \hat{S}_2^z + \hat{S}_1^x \cdot \hat{S}_2^x + \hat{S}_1^y \cdot \hat{S}_2^y) .
\tag{27}$$

The \hat{S}^x and \hat{S}^y operators are expressed in terms of stepping operators,

$$\hat{S}^x = (\hat{S}^+ + \hat{S}^-)/2
\tag{28}$$

and

$$\hat{S}^y = (\hat{S}^+ - \hat{S}^-)/2i .
\tag{29}$$

So that the Hamiltonian becomes,

$$\mathcal{H} = -2J(\hat{S}_1^z \cdot \hat{S}_2^z + \frac{1}{2}(\hat{S}_1^+ \cdot \hat{S}_2^- + \hat{S}_1^- \cdot \hat{S}_2^+)) .
\tag{30}$$

In the absence of the perturbation expressed by this Hamiltonian, the wavefunctions (18) are degenerate, and perturbation theory must be applied to the system (Sherwin, 1961; Eyring, Walter and Kimball, 1944). Thus the 16 matrix elements $(\psi_i | \mathcal{H} | \psi_j)$ must be calculated. The resulting perturbation matrix is

$$\begin{array}{cccc}
 & \psi_1 & \psi_2 & \psi_3 & \psi_4 \\
 \psi_1 & -\frac{1}{2}J & & & \\
 \psi_2 & & \frac{1}{2}J & -J & \\
 \psi_3 & & -J & \frac{1}{2}J & \\
 \psi_4 & & & & -\frac{1}{2}J
 \end{array} \quad (31)$$

This matrix is block diagonal and contains three smaller matrices, two 1×1 matrices and one 2×2 matrix. The 1×1 matrices are trivial and have eigenvalues of $-\frac{1}{2}J$. The 2×2 matrix has two eigenvalues $-\frac{1}{2}J$ and $3/2J$. The diagonalization of the 4×4 matrix is summarized below.

Table 3. Eigenvalues and eigenfunctions for two electron system

Eigenvalue	Eigenfunction	S	S_z
	$\psi_1 = ++\rangle$	1	1
$-\frac{1}{2}J$	$\psi_2 = 1/\sqrt{2}[+-\rangle + -+\rangle]$	1	0
	$\psi_3 = --\rangle$	1	-1
$3/2J$	$\psi_4 = 1/\sqrt{2}[+-\rangle - -+\rangle]$	0	0

The magnetic properties, whether the substance is ferromagnetic or antiferromagnetic, depends on the sign of the exchange constant J . Assume the J is negative and shift the energy levels such that the singlet is at $E = 0$, and then calculate

the magnetic susceptibility of this system ignoring the second order Zeemann term using Equation 23.

$$\chi = \frac{2\beta^2}{kT} \frac{\exp(-2J/kT)}{1 + 3\exp(-2J/kT)}$$

$$\chi = \frac{2\beta^2}{4k[T+J/2k]} \quad (32)$$

since $\exp(2J/kT) \simeq 1 + 2J/kT$ for $2J/kT \ll 1$. It is seen that the magnetic susceptibility is of the form of Equation 24, with $\theta = J/2k$. We have considered only the interaction between two spins but analogous results should be obtained for a more general system (Van Vleck, 1945). The molecular field of Weiss is thus related to the quantum mechanical exchange integral J . What is needed now is some theoretical justification for the Hamiltonian which was used to describe the interaction between spins. This is generally done (Morrish, 1965; Van Vleck, 1945; and Smart, 1966) by considering the interaction between two electrons in two orthogonal orbitals, ψ_a and ψ_b . The Hamiltonian for such a two electron system is given by

$$\mathcal{H} = -\frac{\hbar^2}{2m} \nabla_1^2 - \frac{\hbar^2}{2m} \nabla_2^2 + v(1) + v(2) + \frac{e^2}{r_{12}} \quad (33)$$

$$\mathcal{H} = \mathcal{H}^0 + e^2/r_{12} . \quad (34)$$

where 1 and 2 refer to the coordinates of electron 1 and

electron 2, respectively. The two possible orbital wavefunctions for the system are,

$$\phi_s = 1/\sqrt{2}[\psi_{a(1)}\psi_{b(2)} + \psi_{a(2)}\psi_{b(1)}] \quad (35)$$

and

$$\phi_t = 1/\sqrt{2}[\psi_{a(1)}\psi_{b(2)} - \psi_{a(2)}\psi_{b(1)}] . \quad (36)$$

It is easiest to obtain the energy eigenvalues of \mathcal{H}^0 first and to treat e^2/r_{12} as a perturbation.

$$\mathcal{H}^0 \phi = E^0 \phi \quad (37)$$

yields

$$E^0 = E_a + E_b \quad (38)$$

for both ϕ_s and ϕ_t . The effect of the interaction e^2/r_{12} is to split this degeneracy. Thus,

$$E_s = E^0 + C + J \quad (39)$$

and

$$E_t = E^0 + C - J \quad (40)$$

where

$$C = \langle \psi_{a(1)}^* \psi_{b(2)}^* | e^2/r_{12} | \psi_{a(1)} \psi_{b(2)} \rangle \quad (41)$$

and

$$J = \langle \psi_{a(1)}^* \psi_{b(2)}^* | e^2/r_{12} | \psi_{a(2)} \psi_{b(1)} \rangle . \quad (42)$$

C and J are the Coulomb and exchange integrals. When spin is considered to complete the wavefunctions it is necessary to take cognizance of the Pauli Exclusion Principle and construct only totally antisymmetric wavefunctions. Therefore, we write

$$\phi_s = 1/\sqrt{2}[\psi_{a(1)}\psi_{b(2)} + \psi_{a(2)}\psi_{b(1)}][\alpha(1)\beta(2) - \alpha(2)\beta(1)] \quad (43)$$

$$\begin{aligned} \text{and} & \quad [\alpha(1)\alpha(2)] \\ \emptyset_t = 1/\sqrt{2}[\psi_a(1)\psi_b(2) - \psi_a(2)\psi_b(1)] & \quad [\alpha(1)\beta(2) \pm \alpha(2)\beta(1)] \quad (44) \\ & \quad [\beta(1)\beta(2)] \end{aligned}$$

It is seen that \emptyset_s is a spin singlet and \emptyset_t is a spin triplet. It is also seen that the singlet and triplet are separated in energy by $2J$ by the perturbation e^2/r_{12} , exactly the same result as that obtained with the Hamiltonian given by Equation 25. Thus, this Hamiltonian is a spin Hamiltonian representing the interaction between electrons. This is analogous to the situation in magnetic resonance where a spin Hamiltonian is written which summarizes the effects of the interaction of the spins with the crystal field and the magnetic field.

Van Vleck (1945) has shown that the interaction represented by Equation 25 is general and can be applied to system of many spins. Therefore, for a one-dimensional linear chain of spin $\frac{1}{2}$ ions, such as is found in CsCuCl_3 , we may use

$$\mathcal{H} = -2J \sum_{i=1}^N \hat{S}_i \cdot \hat{S}_{i+1} \quad (45)$$

to represent the exchange coupling between nearest neighbor spins.

Very little progress has been made with this sort of interaction term in two and three dimensions. In the

case of one dimensional infinite linear chains the calculation of the thermodynamic and magnetic properties is not possible. However, Griffiths (1961) and Bonner and Fisher (1964) have made calculations for the eigenvalues and eigenvectors of this Hamiltonian for finite rings of 2 to 11 spin $\frac{1}{2}$ atoms. In using these eigenvalues and eigenvectors to calculate the thermodynamic and magnetic properties of these systems they have been able to show that the properties of the infinite linear chains are well approximated by rings of 10 and 11 atoms for temperatures above $kT/|J| = 1$.

One begins with a chain of two spin $\frac{1}{2}$ atoms, as was done above, and calculates the eigenvalues and eigenvectors of the perturbing Hamiltonian whose general form is

$$\mathcal{H} = -2J \sum_{i=1}^N [\hat{S}_i^z \cdot \hat{S}_{i+1}^z + \frac{1}{2}\gamma(\hat{S}_i^+ \cdot \hat{S}_{i+1}^- + \hat{S}_i^- \cdot \hat{S}_{i+1}^+)] , \quad (46)$$

when the wavefunctions are expressed in terms of the S_z values of the individual atoms. In the case of spin $\frac{1}{2}$ atoms we have two states for each atom + or - corresponding to the eigenvalues $S_z = \pm \frac{1}{2}$.

With $N = 2$ there are four wavefunctions and the perturbation matrix is a 4×4 . With $N = 3$ there are eight wavefunctions and the resulting 8×8 matrix is block diagonal with two

1x1 matrices and two 3x3 matrices. The case of $N = 4$ has been worked out in detail by the author and the results are shown in Appendix II. With a ring of 4 spins the matrix is 16x16 and if states are grouped according to their total S_z values the matrix is nicely block diagonal with two 1x1 matrices, two 4x4 matrices and one 6x6 matrix. This is due to the fact that the S_z commutes with the Hamiltonian given by Equation 46.

As the ring size increases the order of the matrix increases rapidly. For $N = 5$ it is 32, for $N = 6$ it is 64. For $N = 11$ the order is 2028 with the largest S_z blocks having orders of 462. The orders of the various blocks are given below with their S_z values.

S_z	11/2	9/2	7/2	5/2	3/2	1/2	-1/2	-3/2	-5/2
Order	1	11	55	165	350	462	462	330	165

S_z	-7/2	-9/2	-11/2
Order	55	11	1

It is only necessary to diagonalize the matrices for the positive S_z values since the matrices for the negative S_z values are exactly the same. This reduction still leaves some very large matrices to be diagonalized. By making use of the translational invariance of the rings (Bonner, 1968) it is possible to reduce the matrices further. This is best illus-

trated with an example, such as the $S^z = 9/2$ block.

$$\hat{T}|++++-++++\rangle = |++++-++++\rangle \quad (47)$$

\hat{T} is called the translational operator. The resulting wavefunction of this operator differs from the original only in phase. Thus the following statement can be written,

$$\hat{T}\psi_n = \exp(2\pi iq/N)\psi_n, \quad (48)$$

where $q=0,1,2,3,\dots,N-1$. N is the number of atoms in the ring.

Using this technique an 11×11 matrix has been reduced to 11 1×1 matrices, one for each value of q .

The reduction of the other matrices are summarized below.

S_z	11/2	9/2	7/2	5/2	3/2	1/2
Order before Trans. Red.	1	11	55	165	330	462
Order after Trans. Red.	1	1	5	15	30	42

These matrix reductions make it feasible to determine the eigenvalues and eigenvectors of the 2024×2024 matrix with high speed computers. It should be mentioned, however, that it took Bonner six hours of computer time to completely diagonalize this matrix on the University of London Ferranti "Mercury" computer.

Once the eigenvalues are obtained the thermodynamic properties of the rings may be calculated. The eigenvalues with

their S^Z values enable one to calculate the magnetic susceptibilities. If trouble is taken to obtain eigenvectors also, the long- and short-range ordering can be calculated and compared with neutron diffraction experiments.

It is seen, then, that except for the elegant methods by which the original $2^n \times 2^n$ matrix is successively reduced, this is a simple brute force type approach to the thermal and magnetic properties of linear chain ferro- and antiferro-magnets.

The results of calculations for the parallel and perpendicular magnetic susceptibilities using the Bonner-Fisher approach are shown in Figs. 2 and 3, respectively. It is interesting to note that the parallel susceptibility for $\gamma = 1$ does not go to zero as T goes to zero. The perpendicular susceptibility at absolute zero is non-zero for all values of γ .

The method of calculating the parallel susceptibility is outlined in Appendix II. The calculation of the perpendicular susceptibility for rings of 10 and 11 spins is very difficult. Bonner and Fisher used the perpendicular susceptibility for a ring of four spins to estimate the infinite spin perpendicular susceptibility. For $kT/|J| > 1.5$ this is a very good approximation. For $kT/|J| < 1.5$ the susceptibility was estimated by comparison with the Ising model perpendicular susceptibility.

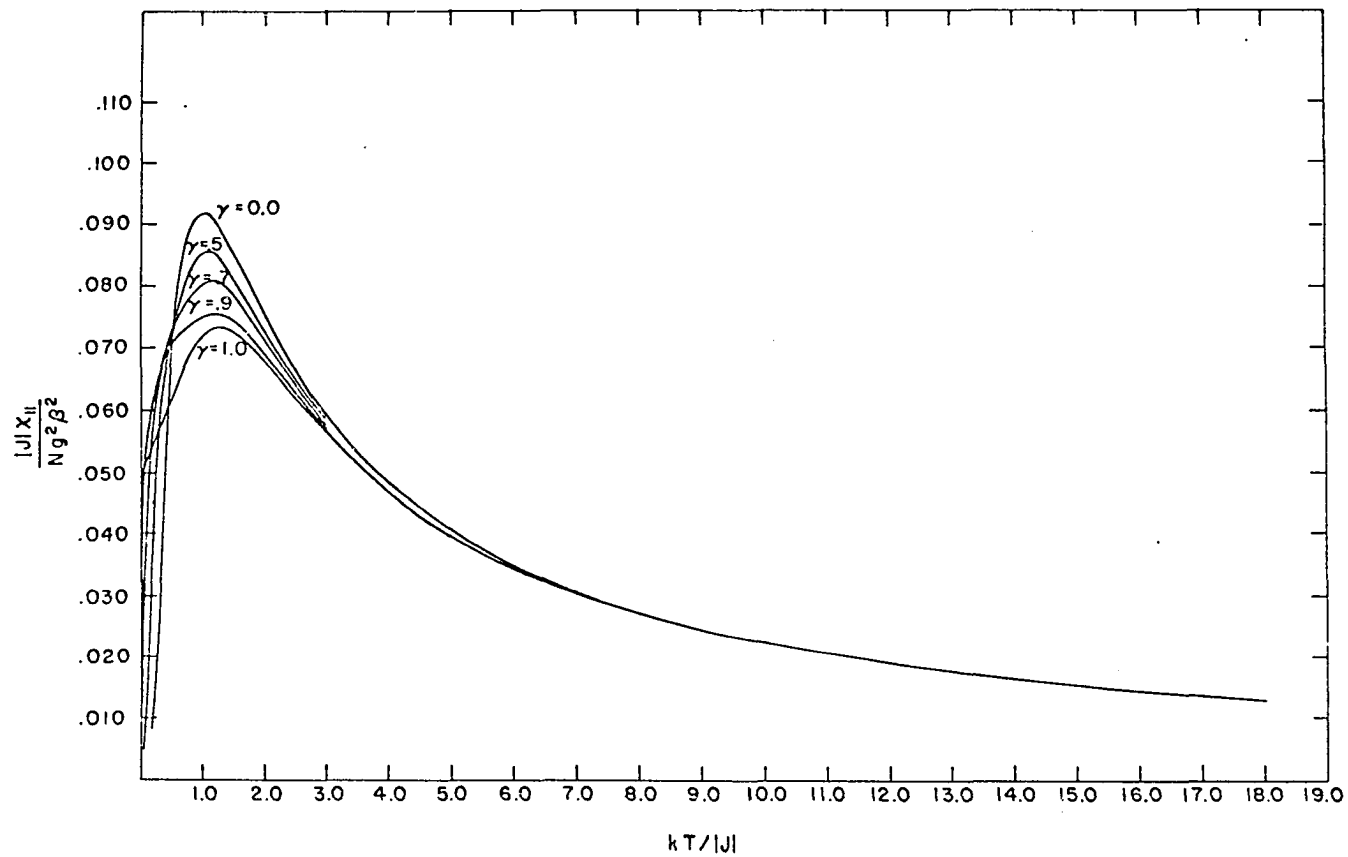


Fig. 2. The parallel susceptibility as a function of γ for a one-dimensional infinite chain spin $\frac{1}{2}$ antiferromagnet

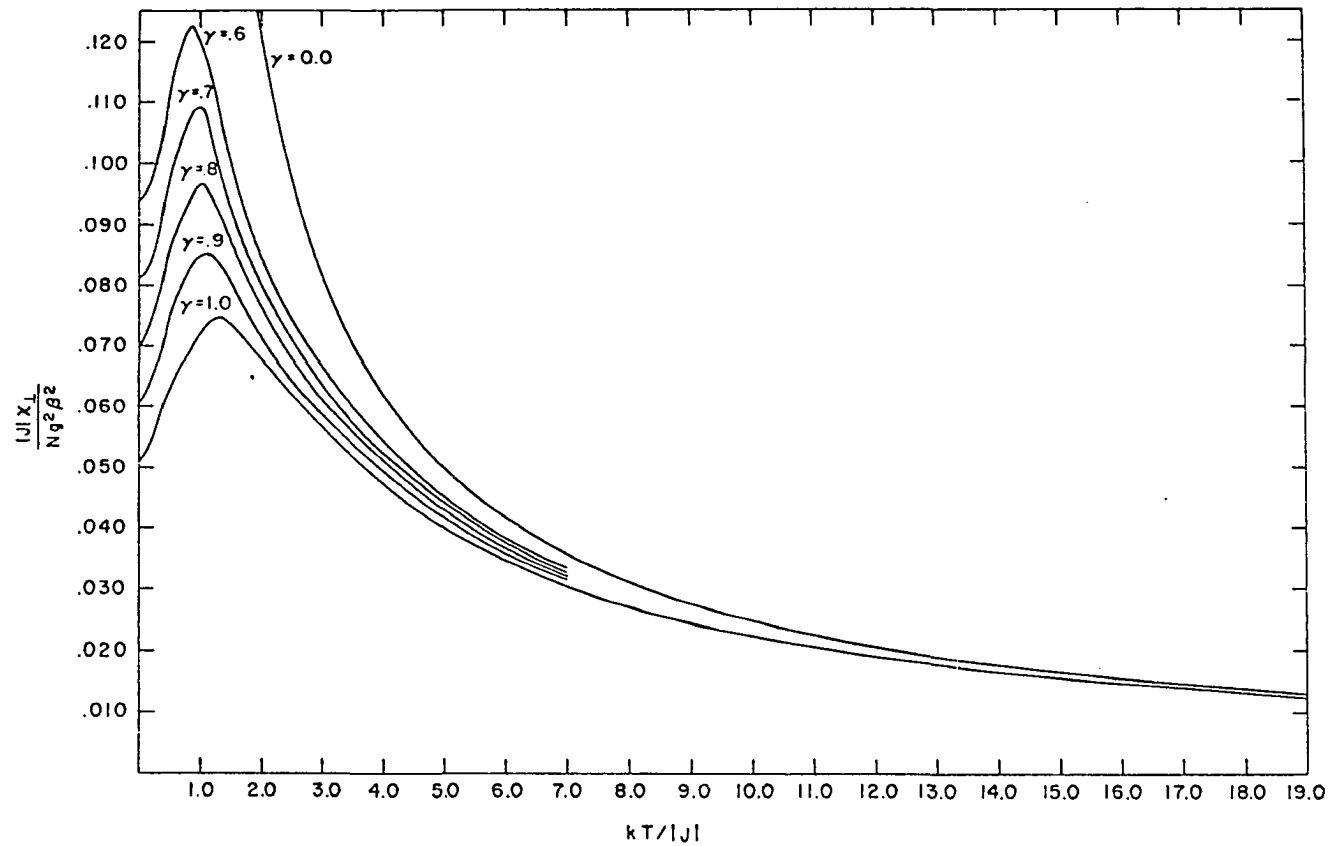


Fig. 3. The perpendicular susceptibility as a function of γ for a one-dimensional infinite chain spin $\frac{1}{2}$ antiferromagnet

EXPERIMENTAL

The single crystal magnetic susceptibility measurements were made employing a modification of the Hartshorn mutual inductance bridge based on the design of Maxwell (1965). The basic components of the Maxwell bridge are shown in Fig. 4.

The basic principle of operation of this type of bridge is that the voltage induced in the secondary circuit of the mutual inductance bridge depends on the permeability of the substance placed in the sample coils. The secondary circuit is balanced with the sample in the coil and out of the coil. The difference in the mutual inductance (voltage) which the ratio transformer must tap off between the "in" and "out" readings is directly related to the magnetic susceptibility. The resistive network shown is required because the voltages induced in the secondary are not pure and have some in-phase character. The resistive network is used to null any in-phase impurity. Without it the bridge could not be balanced. Also, in the measurement of the magnetic susceptibility of ferromagnetic materials, there frequently are magnetic losses which are resistive in nature. The resistive network allows one to obtain quantitative estimates of the losses.

The actual circuit diagram for the mutual inductance

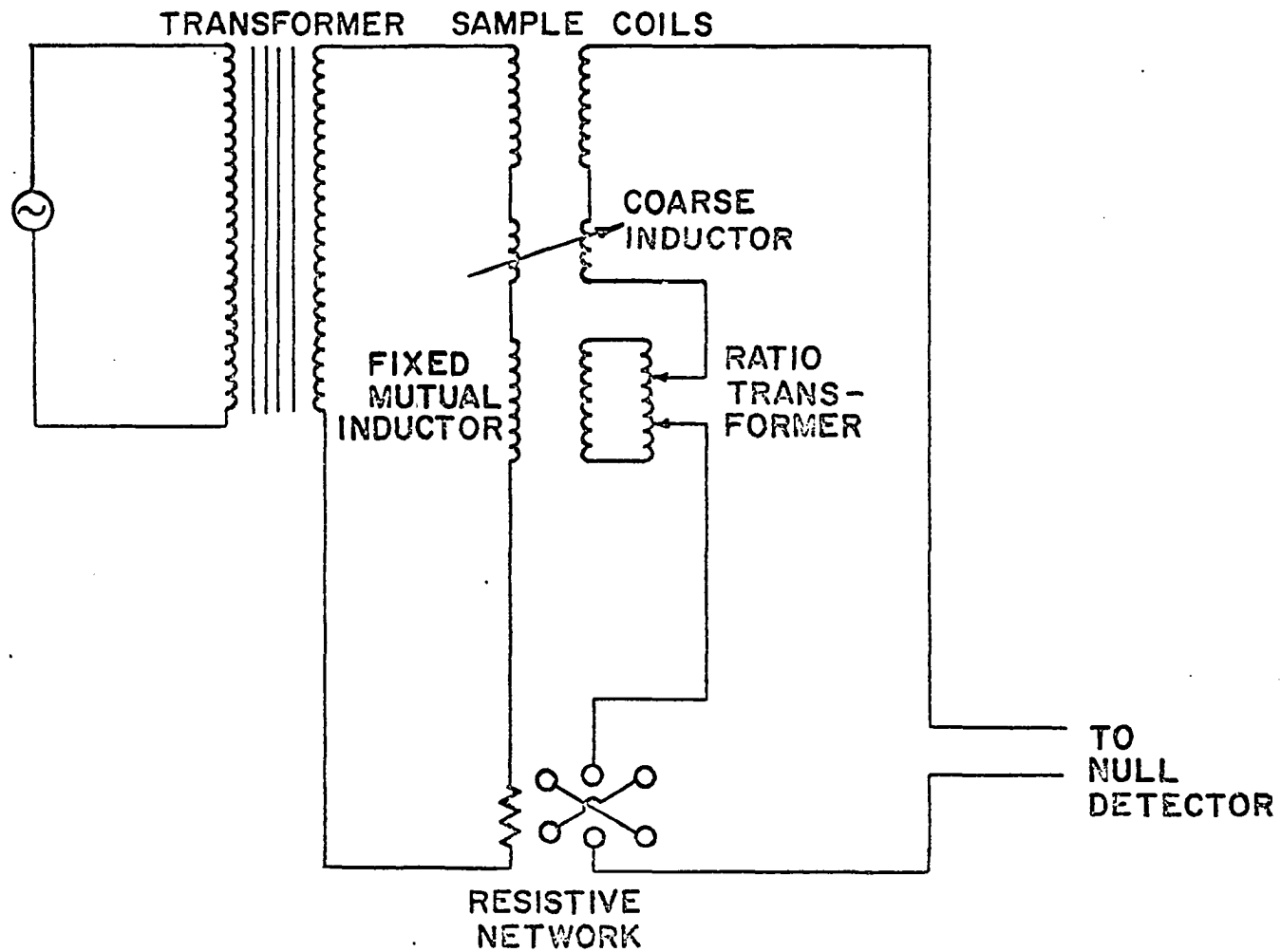


Fig. 4. Circuit diagram for Maxwell's mutual inductance bridge

bridge used in this work is shown in Fig. 5. The primary circuit consists of a 33-cycle generator followed by a power amplifier. In series with the power amplifier and generator are the sample coil primary, the coarse inductor primary, the primary of the fixed mutual inductor, and the resistive network. The 0.1 ohm resistor is common to both the primary and secondary circuits and is, as has been mentioned, necessary to null resistive voltage in the secondary circuit. The secondary circuit consists of the ratio transformer (ESI "Dekatron" model #DT 45) in series with the coarse inductor secondary, the sample coil secondary, the 0.1 ohm resistor and null detector. The null detector is a 33-cycle narrow-band amplifier with an oscilloscope to monitor the signal. The oscilloscope is externally synced to the 33-cycle generator. The generator and detector are contained in one unit, the ESI AC GENERATOR DETECTOR model 861A. This unit has a frequency range from 20 to 20,000 Hz.

The sample coils are wound astatically such that the coupling in the absence of a sample is zero. The basic coil design is shown in Fig. 6. The actual coil has four primary layers of No. 30 wire and three secondary layers of No. 34 wire. Because it is very difficult to wind a perfectly astatic

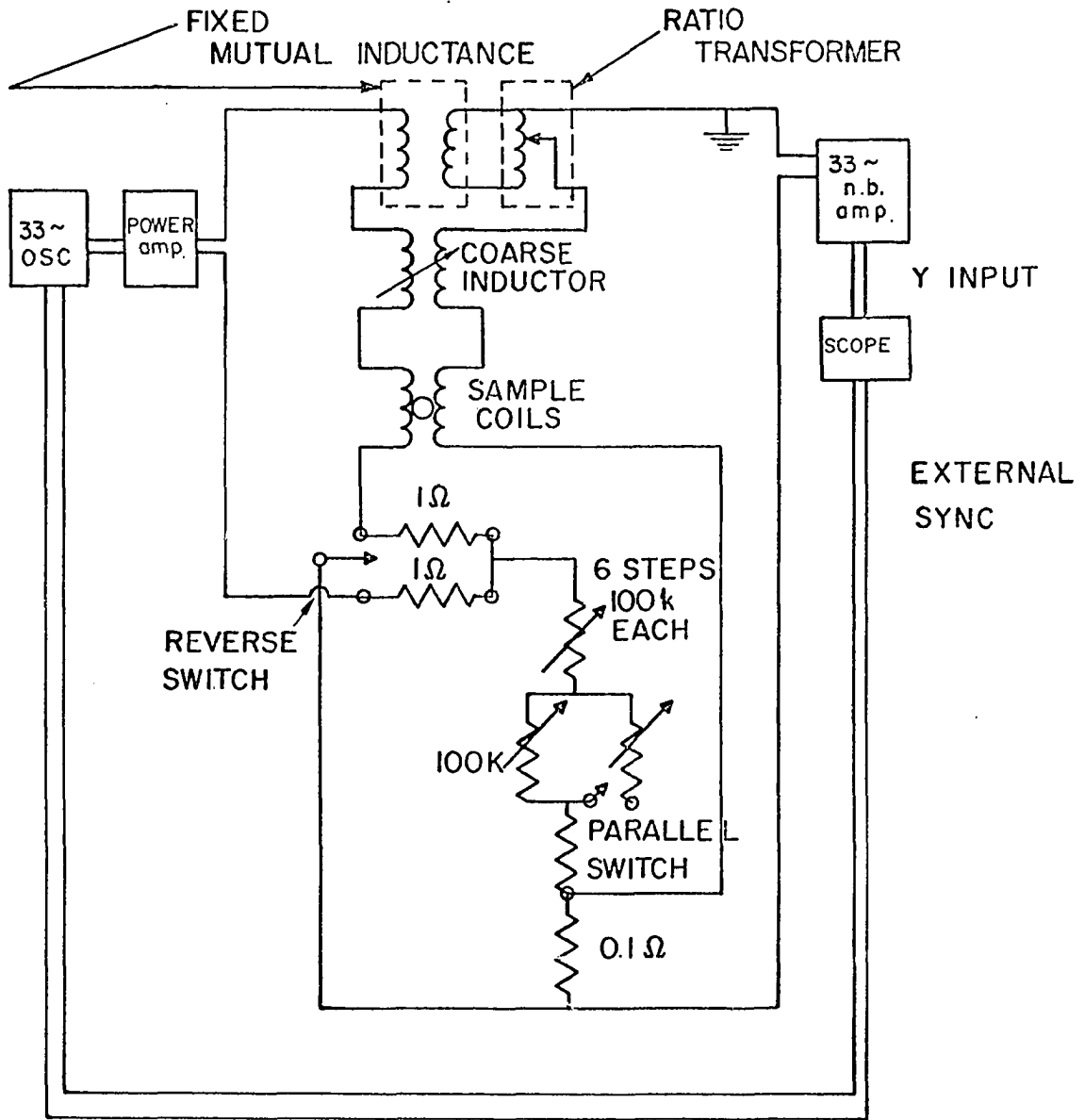


Fig. 5. Circuit diagram for mutual inductance bridge

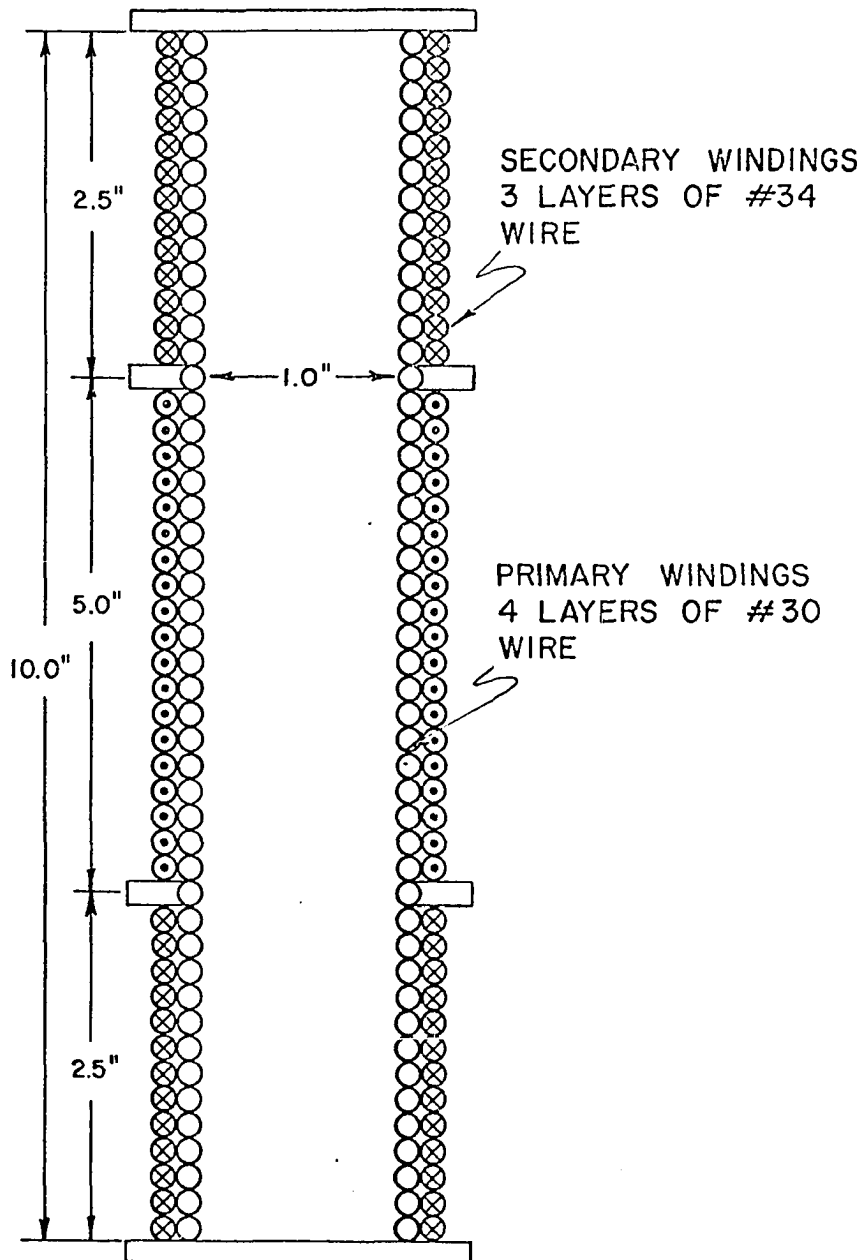


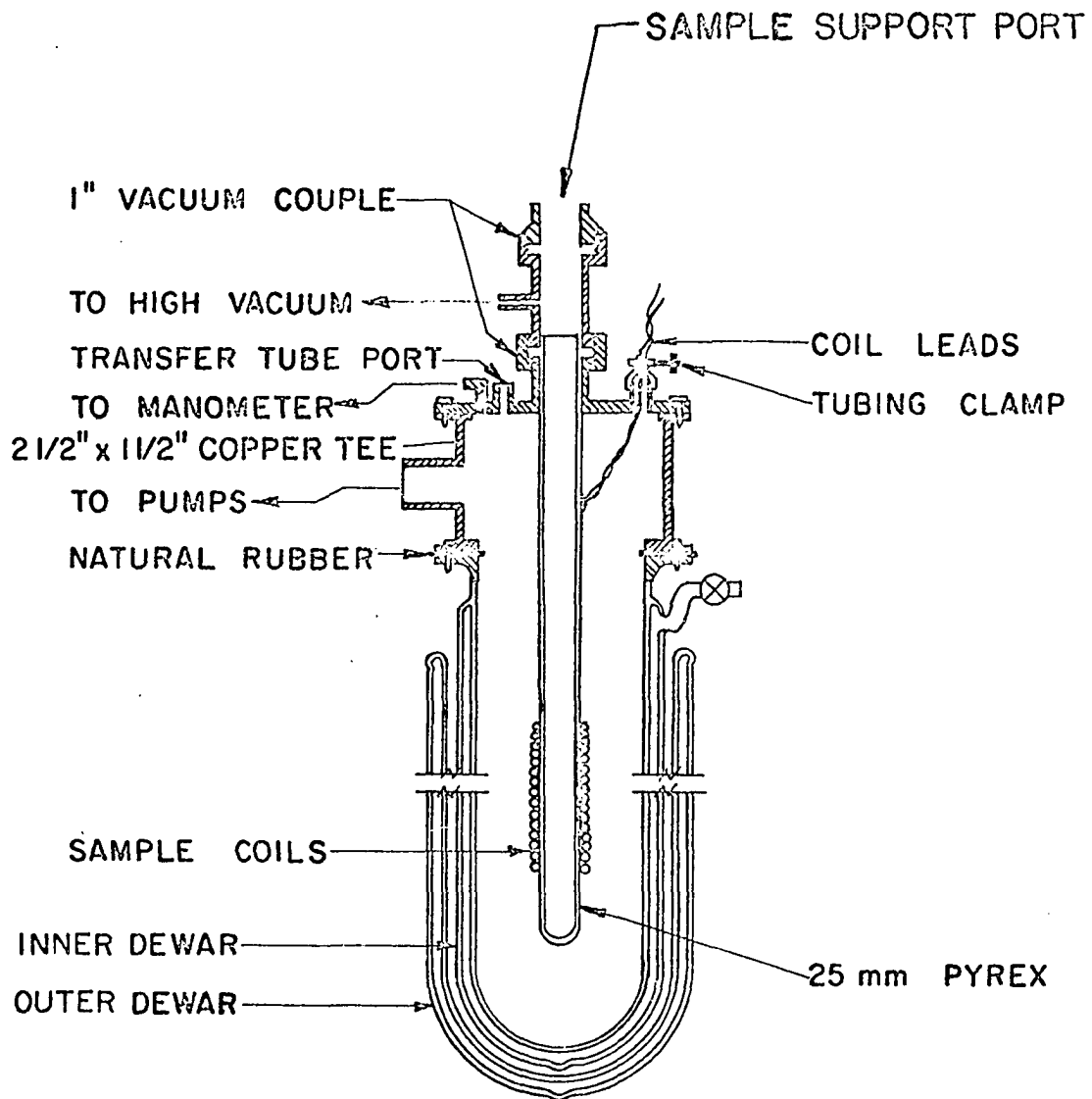
Fig. 6. Sample coils

coil, it is necessary to have a coarse inductor which is used to reduce the signal in the secondary so that it is at a level that can be nulled by the ratio transformer component of the secondary.

The cryostat system and sample support assembly employed are basically the same as those described by Gerstein (1960), as shown in Fig. 7 and Fig. 8, respectively. The single crystal sample holders are shown in greater detail in Fig. 9. The single crystals were attached to the holders with G. E. 7031 adhesive.

Temperatures were measured using a thermocouple constructed of No. 36 B.&S. Au-2%Cu coupled to No. 36 B.&S. Cu wire. The thermocouple was referenced at the ice point of water and was calibrated at 4.2°K against ⁴He vapor pressure for each helium run.

The sample coil was calibrated using Gd₂O₃ at 4.2° and 77.3°K. The original magnetic susceptibility measurements on Gd₂O₃ were performed by Miller and Jelinek (1968) of this laboratory. We estimate that our measurements are accurate to within 1% in the liquid helium range (1.3° to 77.3°K) and to within 2% in the liquid nitrogen range (77.3° to 140°K).



CRYOSTAT SYSTEM

Fig. 7. Cryostat system

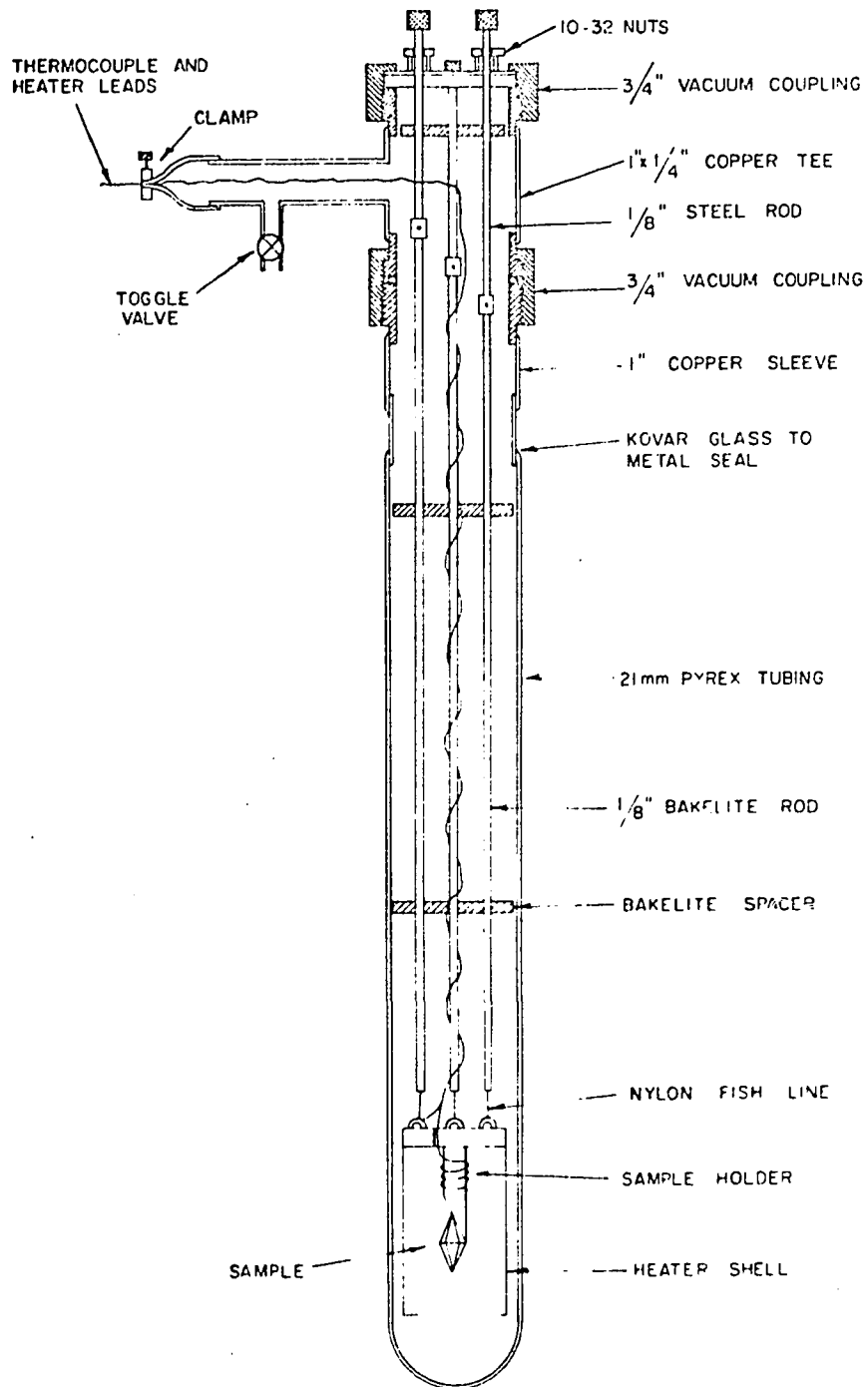


Fig. 8. Sample support assembly

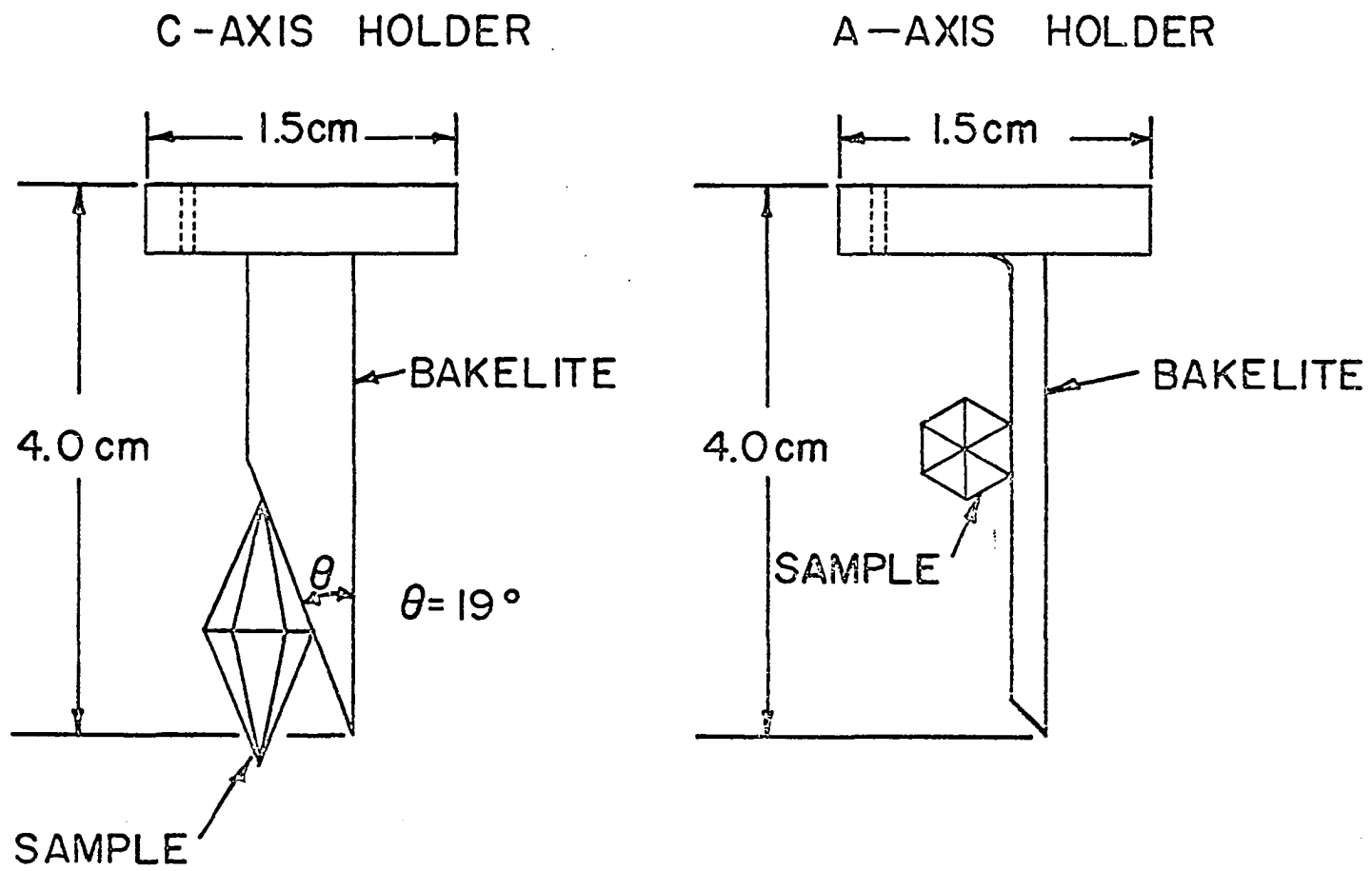


Fig. 9. Sample holders for the c- and a-axes

Single Crystal Data

Magnetic susceptibility measurements were made with the magnetic field parallel to the crystallographic c- and a-axes. The c-axis is parallel to the direction of the infinite chains of copper atoms. The a-axis is perpendicular to the chain direction.

Three different single crystals were used in making measurements. Two crystals weighing 2.1733 g and 1.8096 g were used in making c-axis measurements. The third crystal weighing 1.6846 g was used in a-axis measurements. Chemical analysis was performed on the crystal weighing 1.8096 g and it was found to contain $20.93 \pm .03\%$ copper. The theoretical percentage is 20.98%. The analysis performed was iodometric titration of the copper ions.

The single crystals were grown from an aqueous solution of CsCl and $\text{CuCl}_2 \cdot 2\text{H}_2\text{O}$ containing a 5% excess of $\text{CuCl}_2 \cdot 2\text{H}_2\text{O}$ to prevent precipitation of Cs_2CuCl_4 . The crystals grew as hexagonal bipyramids with $(10\bar{1}1)$ faces. The single crystal data are presented numerically in Tables 4 and 5 and graphically in Figs. 9, 10 and 11.

Table 4. A-axis magnetic susceptibilities (exp. values)

T ^o K	χ	T ^o K	χ	T ^o K	χ
1.83	.0209510	24.09	.0157200	77.62	.0063740
2.38	.0204810	25.34	.0150830	80.32	.0061740
2.84	.0203820	26.21	.0149300	82.41	.0060850
3.41	.0202610	27.72	.0146600	83.05	.0059760
3.88	.0206600	27.63	.0145200	85.10	.0058540
4.18	.0202160	27.94	.0145000	89.02	.0056370
4.18	.0205190	28.85	.0142100	92.48	.0054120
4.73	.0202300	29.19	.0141200	92.48	.0054220
5.44	.0201370	29.74	.0138800	92.48	.0054050
6.30	.0203400	30.34	.0137200	95.86	.0052790
6.90	.0205000	31.04	.0136500	95.86	.0052430
7.57	.0205100	32.30	.0133600	95.86	.0052160
8.84	.0205000	33.94	.0129400	97.38	.0051660
8.93	.0203600	35.53	.0125600	97.38	.0051880
9.00	.0205200	35.92	.0124800	98.39	.0050820
9.52	.0205000	37.45	.0122200	98.39	.0051950
9.71	.0204600	39.69	.0116500	98.39	.0051950
10.24	.0205000	41.85	.0112100	100.90	.0050400
10.89	.0200900	43.67	.0099700	100.90	.0050470
11.78	.0199500	49.95	.0095930	104.90	.0048980
12.12	.0191920	52.19	.0082980	105.59	.0048370
12.12	.0191920	54.38	.0089440	109.28	.0046700
12.26	.0191400	57.14	.0084740	112.29	.0045350
13.09	.0185130	60.14	.0081400	115.44	.0044640
15.55	.0182740	61.61	.0080870	117.90	.0043410
16.42	.0180200	61.61	.0080870	118.46	.0042820
17.22	.0177000	63.08	.0077200	118.46	.0043310
19.28	.0168700	65.52	.0074920	122.80	.0041910
19.68	.0169300	66.54	.0073640	128.34	.0040150
20.19	.0167200	69.36	.0070860	132.84	.0038750
20.56	.0165600	72.15	.0068080	140.11	.0037370
21.55	.0162400	74.90	.0066020	144.34	.0036220
21.89	.0163400				
23.04	.0159100				
23.72	.0157300				

Table 5. C-axis magnetic susceptibilities (exp. values)

T°K	χ	T°K	χ	T°K	χ
1.39	.0177800	43.92	.0097720	98.55	.0045210
2.76	.0177800	43.92	.0098440	102.31	.0044120
2.70	.0179920	46.00	.0093070	104.80	.0041500
3.50	.0176600	48.00	.0090950	104.80	.0041230
3.88	.0179120	49.91	.0086310	106.42	.0043090
4.18	.0177860	52.50	.0082400	106.42	.0043090
4.93	.0176470	55.62	.0077430	107.03	.0040640
7.40	.0177860	58.65	.0073450	107.03	.0040810
8.20	.0179120	61.91	.0070030	107.03	.0041900
9.03	.0180580	65.10	.0067190	107.03	.0042000
9.80	.0178300	67.94	.0064460	108.51	.0040370
10.35	.0176930	71.54	.0062310	110.97	.0039780
10.89	.0175940	71.54	.0062000	111.98	.0039640
12.25	.0173950	74.90	.0059640	111.98	.0039640
13.13	.0171760	77.14	.0056240	111.98	.0039640
14.29	.0167650	77.14	.0056350	113.66	.0039180
15.26	.0165230	78.16	.0056980	116.97	.0038450
15.98	.0163480	79.83	.0055290	116.97	.0038870
16.81	.0162080	79.83	.0054760	116.97	.0038180
17.80	.0159700	79.83	.0054630	117.97	.0037560
18.43	.0157740	81.69	.0054090	119.24	.0037790
19.36	.0154090	83.08	.0053340	120.97	.0035930
20.25	.0152470	83.08	.0053360	120.30	.0035730
21.13	.0150110	84.83	.0051580	120.30	.0036330
22.00	.0149820	85.71	.0052210	121.66	.0036750
24.60	.0140930	85.71	.0051770	125.02	.0035310
26.06	.0136090	87.98	.0049480	127.51	.0034230
27.48	.0131860	88.84	.0050160	127.51	.0034070
28.37	.0127900	91.09	.0048000	128.30	.0034340
30.39	.0124300	91.09	.0048450	132.00	.0033310
32.39	.0119330	91.93	.0048990	133.37	.0033410
34.34	.0115740	91.93	.0048720	143.92	.0098440
41.75	.0102490	95.27	.0046400		

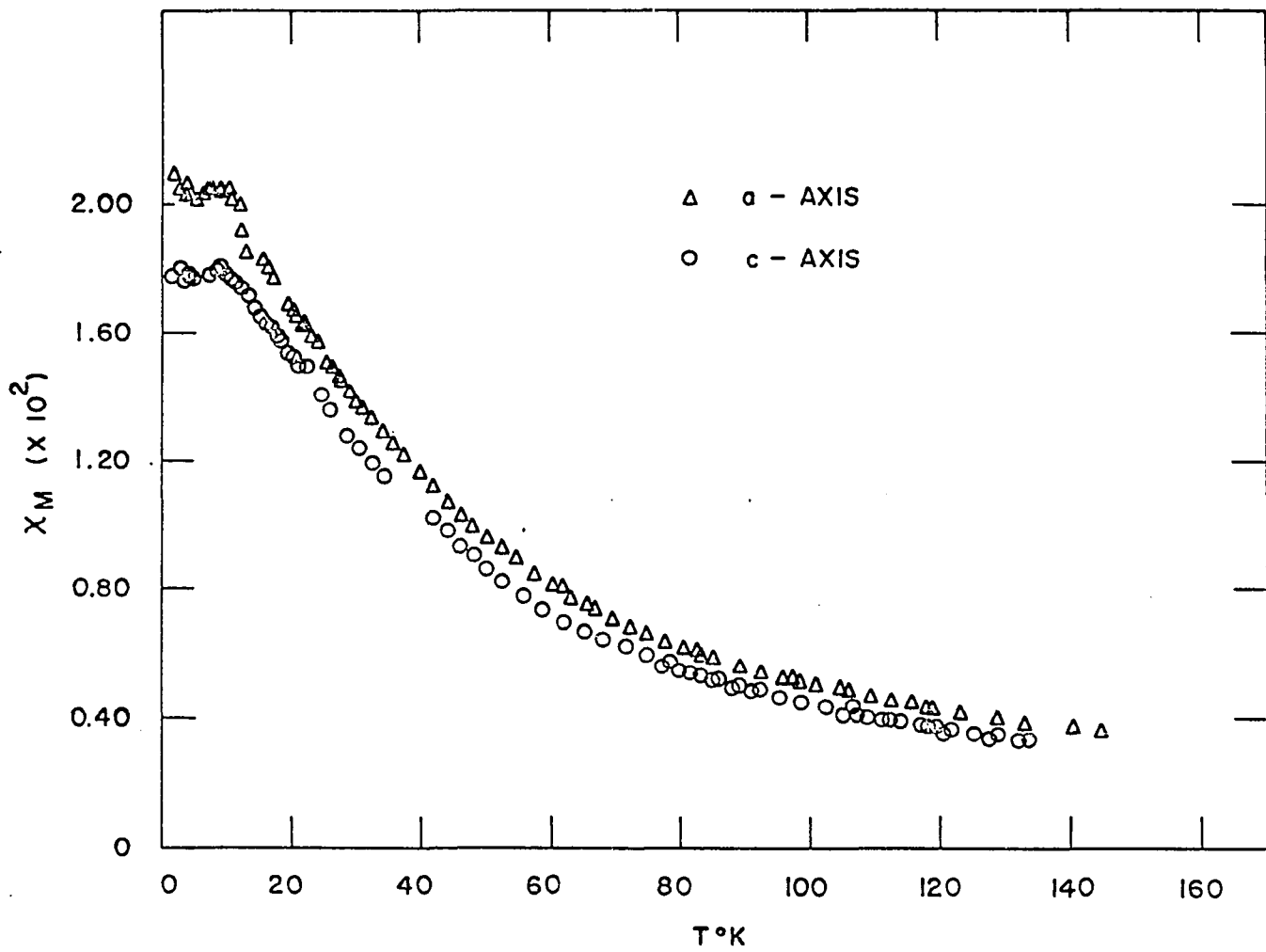


Fig. 10. χ_M as a function of temperature for the a- and c-axes

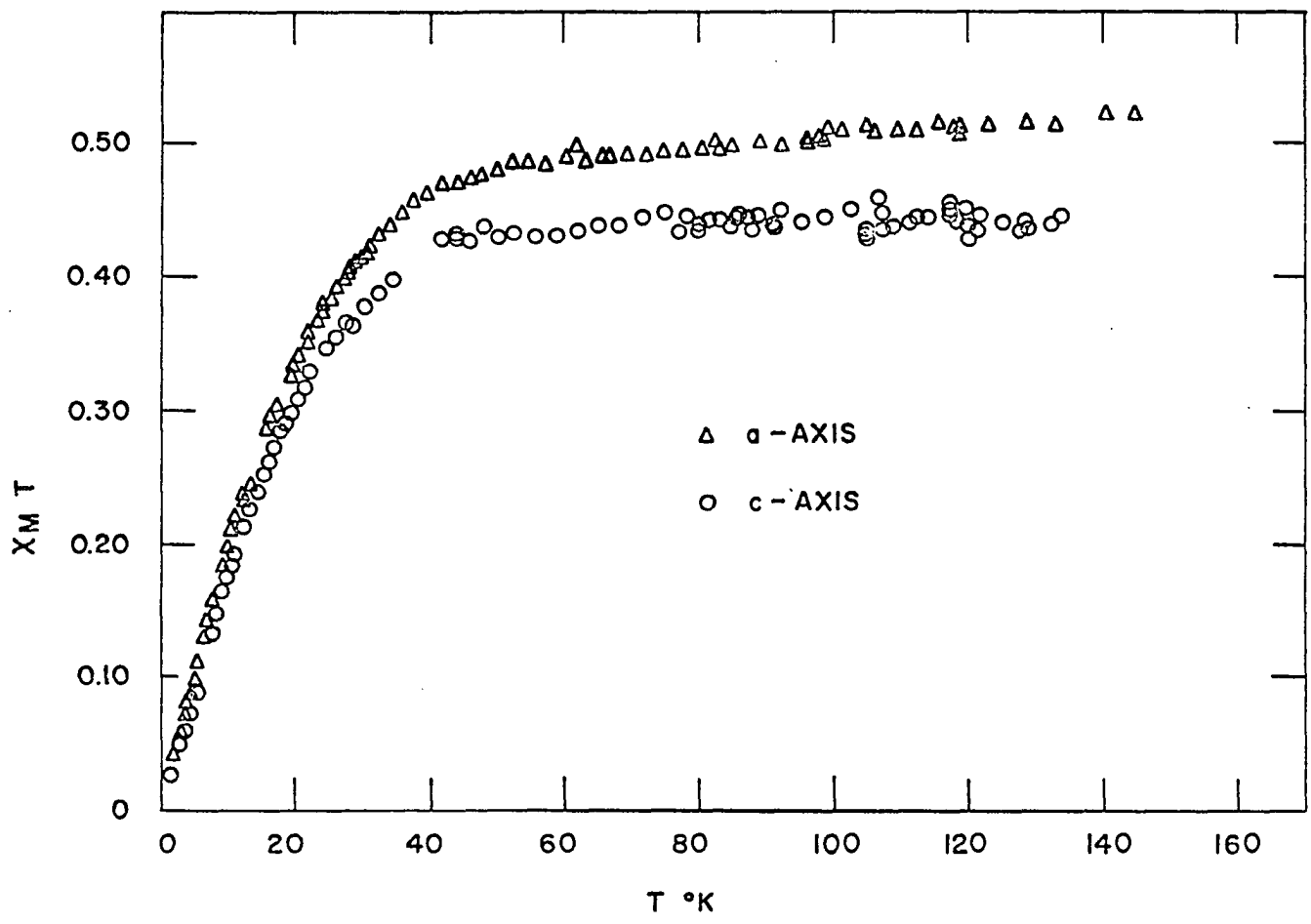


Fig. 11. $\chi_M T$ as a function of temperature for the a- and c-axes

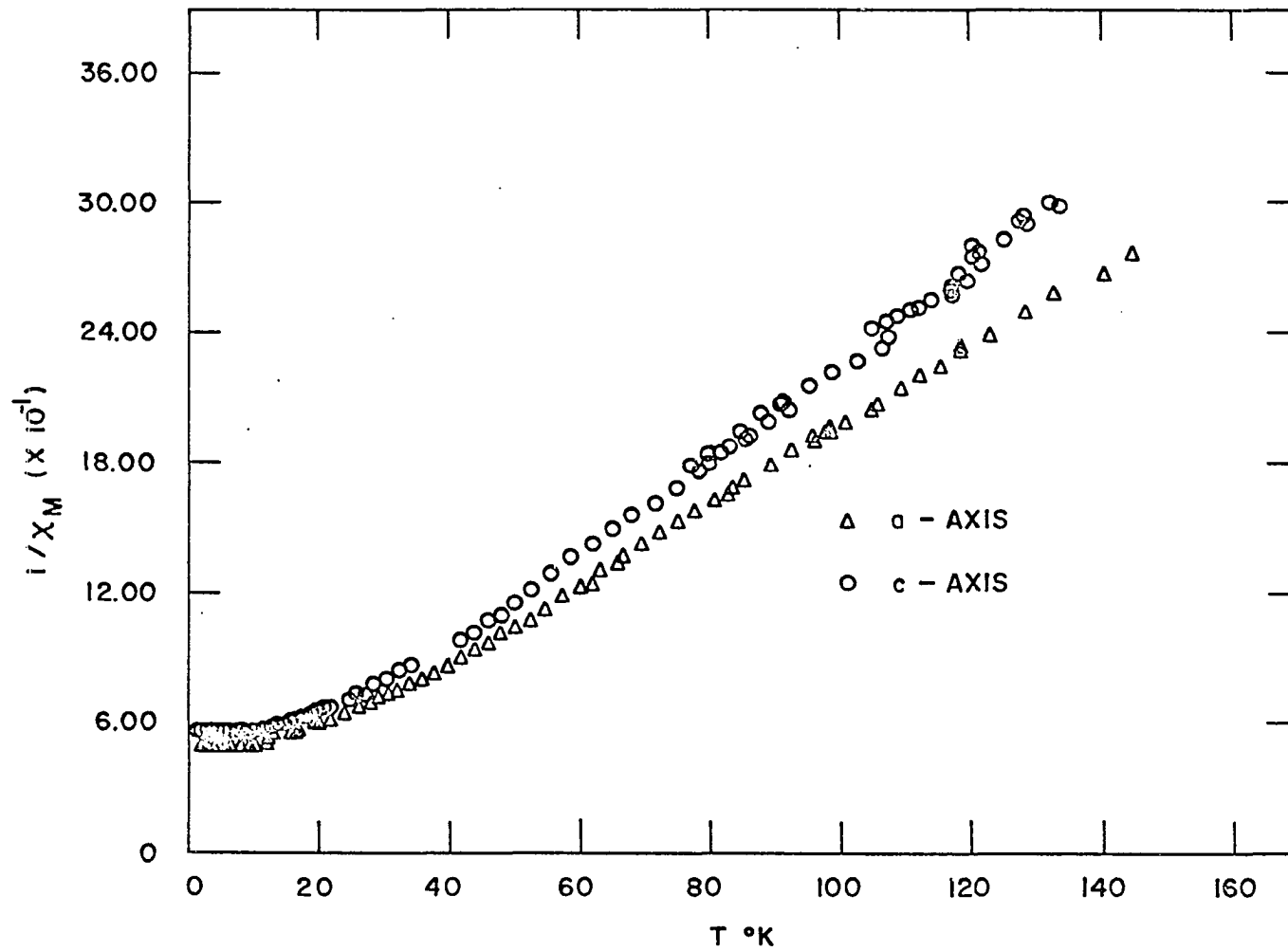


Fig. 12. $1/X_M$ as a function of temperature for the a- and c-axes

DISCUSSION OF RESULTS

Bonding

Figure 11 indicates that deviations from Curie-Law behavior begin at approximately 55°K. Therefore, a least squares refinement of χT vs. T was carried out using only data above 70°K. This analysis gives values for the Curie constant, C , and the temperature independent susceptibility, χ_{TIP} . The susceptibility is then corrected for the temperature independent term and a least squares refinement of $1/\chi$ vs T is performed to obtain the Weiss constant, θ . All least squares analyses were performed on an IBM 360/65 computer, using programs written by the author. The results of the least squares analyses are given in Table 6.

Table 6. Results of least squares analyses

	C Curie const.	Weiss const.	χ_{TIP}	Std. dev. of χT	Std. dev. of $1/\chi$	Averaged Curie const.	Powder Curie const.
A-axis	.464	0.03	400×10^{-6}	.003	1.45	.458	.458
C-axis	.445	.029	10×10^{-6}	.007	3.48		

As can be seen from Table 6 the averaged single crystal g-factors agree very well with the powder data taken previously (Rioux and Gerstein, 1969), which in turn agree closely with

the work of Figgis and Harris (1959) on powder CsCuCl_3 . The Weiss constants obtained here are also in line with the value of $\theta = 1 \pm 1$ of Figgis and Harris.

Our picture of CsCuCl_3 has been to consider each copper to be coordinated D_{4h} to chlorine atoms (Rioux and Gerstein, 1969). The tetragonal axis of the square planar complex involves two non-bonding chlorines which are $2.776\overset{\circ}{\text{Å}}$ from the copper atom. The other four chlorines in the coordination sphere (two at $2.281\overset{\circ}{\text{Å}}$ and two at $2.355\overset{\circ}{\text{Å}}$) are considered, to a first approximation to form a square plane.

A molecular orbital approach to such a square planar complex yields the energy level diagram (Ballhausen and Gray, 1964) shown in Fig. 13. The molecular orbitals corresponding to this diagram are given in Appendix III. After the spin-orbit perturbation is considered the ground state wavefunctions for the system are (Rioux and Gerstein, 1969)

$$\phi_1 = |\phi_{x^2-y^2}^+\rangle - \frac{\alpha\gamma\lambda}{E_{xy}} |\phi_{xy}^+\rangle - \frac{\alpha\gamma\lambda}{2E_{xz}} [|\phi_{xz}^-\rangle - |\phi_{yz}^-\rangle] \quad (49)$$

and

$$\phi_2 = |\phi_{x^2-y^2}^-\rangle + \frac{\alpha\gamma\lambda}{E_{xy}} |\phi_{xy}^-\rangle - \frac{\alpha\gamma\lambda}{2E_{xz}} [|\phi_{xz}^+\rangle + |\phi_{yz}^+\rangle]. \quad (50)$$

Calculations for g_{\parallel} and g_{\perp} of the square planar complex using these ground state wavefunctions yield

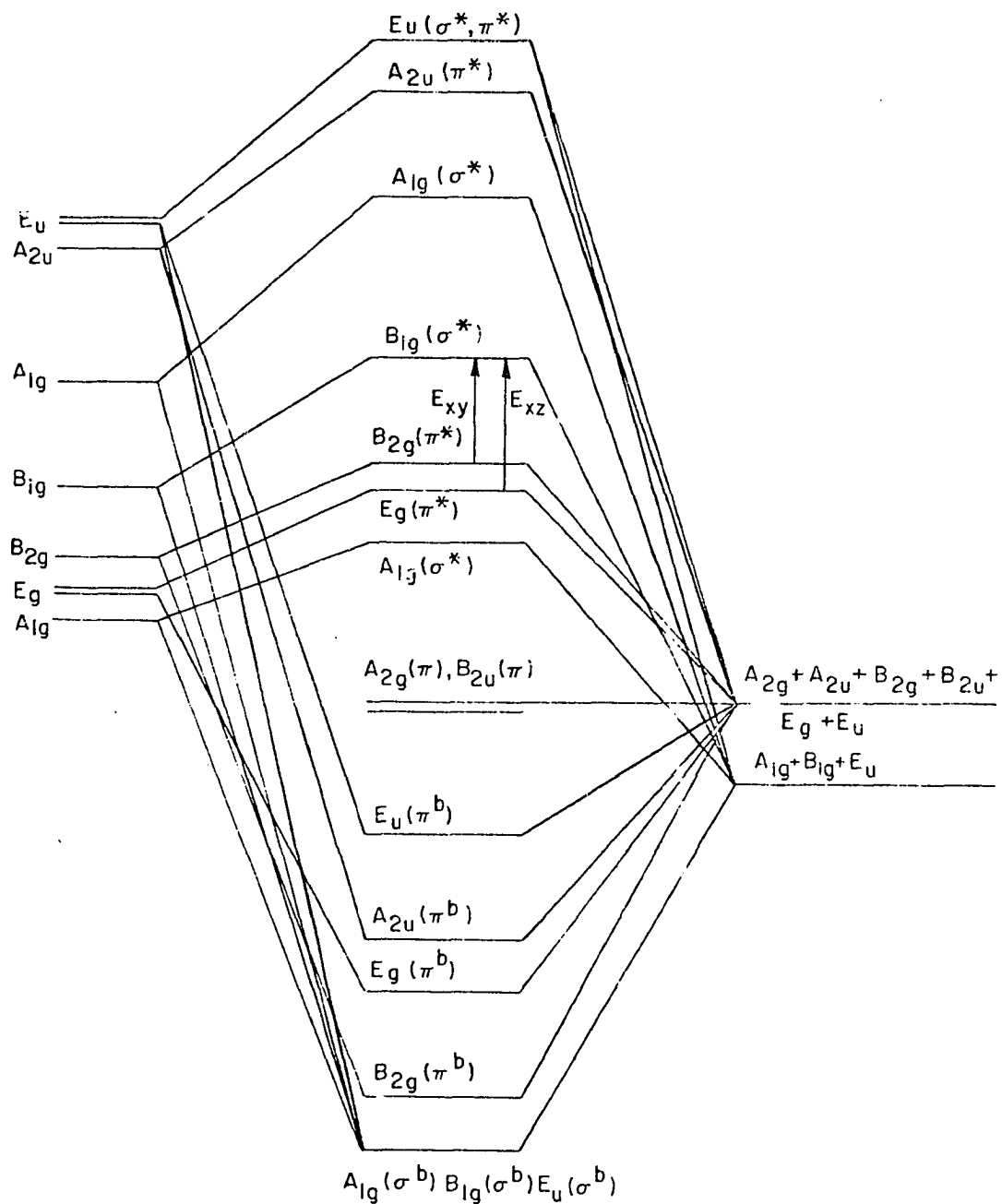


Fig. 13. Molecular orbital diagram for the square planar $CuCl_4^{2-}$ complex

$$g_{\parallel} = 2 \left(1 - \frac{4\alpha^2 \gamma^2 \lambda}{E_{xy}} \right)^2 \quad (51)$$

and

$$g_{\perp} = 2 \left(1 - \frac{\alpha^2 \gamma^2 \lambda}{E_{yz}} \right)^2 \quad (52)$$

Here, λ is the spin-orbit coupling constant which for copper has the value of -830 cm^{-1} . E_{xy} and E_{yz} are shown in Fig. 13. The magnitudes of these energy differences are taken from the spectral study of Day (1964) and have the values $11,000 \text{ cm}^{-1}$ and $11,800 \text{ cm}^{-1}$, respectively. The α^2 and γ^2 are bonding parameters (see Appendix III).

The g_{\parallel} and g_{\perp} calculated above refer to the square planar complexes. They are the g-factors along the molecular tetragonal axis and in the square plane, respectively. In order to correlate g_{\parallel} and g_{\perp} with the g-factors along the c and a crystallographic axes, g_c and g_a , it is necessary to determine the orientation of the square planar complexes with the a- and c-axes.

The final atom position parameters for CsCuCl_3 are given in Table 7 (Schleuter et al., 1966). The lattice parameters are $a = b = 7.2157 \pm 0.0005$ and $c = 18.1777 \pm 0.0010 \text{ \AA}$. The space group is $P6_122$ and the atom positions for all atoms in a unit cell are given in Table 8. The site symmetry of the

Table 7. Final atom position parameters for CsCuCl₃

Atom	x/a	y/b	z/c
Cs	0.35458	0.70916	0.2500
Cu	0.0616	0.000	0.000
Cl(1)	0.8877	0.7754	0.254
Cl(2)	0.3540	0.2095	0.2418

Table 8. Atom positions for space group P₆₁22 (Henry and Lonsdale, 1965)

Twelve chlorine atoms (six pairs of Cl (2) and Cl(2')) at:

x, y, z	;	\bar{y} , x-y, 1/3+z	;	y-x, \bar{x} , 2/3+z
\bar{x} , \bar{y} , 1/2+z	;	y, y-x, 5/6+z	;	x-y, x, 1/6+z
y, x, 1/3-z	;	\bar{x} , y-x, 2/3-z	;	x-y, \bar{y} , \bar{z}
\bar{y} , \bar{x} , 5/6-z	;	x, x-y, 1/6-z	;	y-x, y, 1/2-z

Six chlorine atoms (six Cl(1) atoms) and six Cs atoms at:

x, 2x, 1/4	;	2 \bar{x} , \bar{x} , 7/12	;	x, \bar{x} , 11/12
\bar{x} , 2 \bar{x} , 3/4	;	2x, x, 1/12	;	\bar{x} , x, 5/12

Six copper atoms at:

x, 0, 0	;	0, x, 1/3	;	\bar{x} , \bar{x} , 2/3
\bar{x} , 0, 1/2	;	0, \bar{x} , 5/6	;	x, x, 1/6

copper atoms along the 6-fold screw axis is shown in Fig. 1.

To determine the orientation of the copper complexes it is necessary to determine the angle that the tetragonal axis makes with the a-b plane. The coordinates of Cl(2') in Fig. 1 are $y, x, 1/3-z$, where $x = .3540a$, $y = .2095b$ and $z = .2418c$. The z-coordinate of Cl(2') is, therefore, $1/3-z = .0915$, so that Cl(2') is 0.0915×18.1777 or $1.667\overset{\circ}{\text{Å}}$ above the a-b plane. Therefore, the tetragonal axis makes an angle, θ , of 37° with the plane, since $\sin\theta = 1.667/2.776$.

We may describe the structure of CsCuCl_3 as square planar coordinated coppers with six such complexes in a unit cell. The tetragonal axes of the complex make an angle of 37° with the a-b plane. Looking along the crystallographic c-axis we may say that each complex is roughly $3\overset{\circ}{\text{Å}}$ above the one below it and the projection of its tetragonal axis in the a-b plane is rotated 60° counterclockwise relative to the one below it.

Since all complexes are oriented the same with respect to the c-axis, there exists the following relationship between g_c^2 and g_{\parallel}^2 and g_{\perp}^2 :

$$g_c^2 = \sin^2\theta g_{\parallel}^2 + \cos^2\theta g_{\perp}^2 \quad (53)$$

$$g_c^2 = 0.36 g_{\parallel}^2 + 0.64 g_{\perp}^2 \quad (54)$$

The relationship between g_a^2 , g_{\parallel}^2 and g_{\perp}^2 is slightly more

difficult to obtain. The value of the g-factor in the a-b plane is isotropic for hexagonal systems. For simplicity, then, consider that the field is parallel to the a-b plane and in a direction such that it is parallel to the projection of the tetragonal axes of the first and fourth CuCl_4^- complexes onto the a-b plane. To determine their contribution to g_a^2 we project g_{\parallel}^2 and g_{\perp}^2 on to the a-b plane and weight this projection 1/3. For the four remaining complexes, the tetragonal axis makes an angle of 60° with the magnetic field. Thus, to determine their contribution to g_a^2 we project g_{\parallel}^2 and g_{\perp}^2 onto the a-b plane and then project this projection onto the direction of the magnetic field. This contribution is weighted 2/3. Thus,

$$g_a^2 = 1/3[\cos^2\theta g_{\parallel}^2 + \sin^2\theta g_{\perp}^2] + 2/3[\cos^2 60 (\cos^2\theta g_{\parallel}^2 + \sin^2\theta g_{\perp}^2) + \sin^2 60 g_{\perp}^2] \quad (55)$$

In summary, we have

$$g_c^2 = .36g_{\parallel}^2 + 0.64g_{\perp}^2 \quad (56)$$

$$g_a^2 = .32g_{\parallel}^2 + 0.68g_{\perp}^2 \quad (57)$$

The experimental Curie constants for the a- and c-axes are 0.464 and 0.445, respectively. Thus, $g_a^2 = 4.93$ and $g_c^2 = 4.74$.

If the values of g_{\parallel} (2.44) and g_{\perp} (2.10) estimated from the powder magnetic susceptibility (Rioux and Gerstein, 1969), are used in Equations 56 and 57 the calculated values for g_a^2 and g_c^2 are, $g_a^2 = 4.84$ (experiment 4.93) and $g_c^2 = 4.91$ (experiment 4.74). Our experimentally determined Curie constant for the c-axis is 3% too high and that for the a-axis is 2% too low, if we are to have exact agreement with the previously discussed model. It is interesting to note that if Wells' (1947) original parameters are used to calculate the relations between g_a , g_c , and g_{\parallel} and g_{\perp} better agreement is obtained. In this case the experimental g_a^2 is less than 1% too low and the experimental g_c^2 is 2% too high.

Linear Antiferromagnetism

Examination of the structure of CsCuCl_3 reveals the existence of infinite linear chains of copper ions along a six-fold screw axis centered about the crystallographic c-axis. The coppers are connected by symmetrical Cu-Cl-Cu bridges with Cu-Cl distances of $2.355(4) \text{ \AA}$. The Cu-Cl-Cu angle is 73.8° . There are four chains per unit cell, located at the corners of the unit cell and, therefore, the shortest distance between neighboring chains is 7.20 \AA . This is also

be the shortest possible distance between copper atoms on neighboring chains. The next-nearest chain is at a distance of 12.50\AA (see Fig. 14). It would seem that the one-dimensional interactions between nearest neighbor copper atoms on the infinite chains should predominate over the weaker interchain interactions. This conclusion is reached by considerations of Cu-Cu distances and also by considerations of mechanism for interaction. The symmetric chlorine bridges obviously provided a suitable super-exchange mechanism for one-dimensional coupling with the chain. The interchain exchange interaction appears to be a bit more subtle.

It would appear that initial deviations from paramagnetic behavior in CsCuCl_3 should be explained on the basis of one-dimensional interactions. It is not surprising that the system eventually orders three dimensionally due to the weaker interchain interactions. This type of behavior is not uncommon to one-dimensional copper systems (CuCl_2 , Stout and Chisholm, 1962; $\text{Cu}(\text{NH}_3)_4\text{SO}_4$, Haseda and Miedema, 1961).

Because of the structural evidence for infinite one-dimensional chains of copper ions in CsCuCl_3 we decided to compare our magnetic susceptibility measurements with the calculations of Bonner and Fisher (1964). These calculations (see Appendix II) are based on a model which assumes that the spin $\frac{1}{2}$ atoms

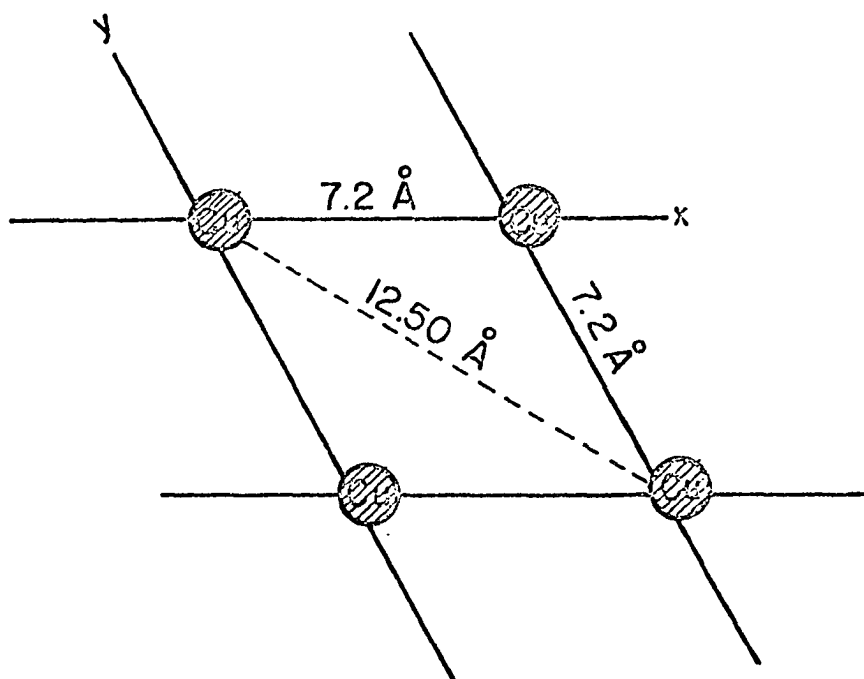


Fig. 14. Relative position of infinite chains in unit cell

forming an infinite linear chain are coupled to their nearest neighbors by an anisotropic Heisenberg interaction,

$$\mathcal{H} = -2J \sum_{i=1}^N (\hat{S}_i^z \cdot \hat{S}_{i+1}^z + \gamma (\hat{S}_i^x \cdot \hat{S}_{i+1}^x + \hat{S}_i^y \cdot \hat{S}_{i+1}^y)) \quad (58)$$

Bonner and Fisher have calculated the parallel and perpendicular susceptibility for various values of γ . The smaller the value of γ the larger the anisotropy in the coupling of the spins. When $\gamma = 0$ we have the completely anisotropic Ising interaction, when $\gamma = 1$ the completely isotropic Heisenberg interaction. The results of the Bonner-Fisher calculations have been previously shown graphically in Figs. 2 and 3.

To compare our experimental magnetic susceptibilities with theory, we have plotted the reduced magnetic susceptibility, $|J|\chi/Ng^2\beta^2$, vs. the reduced temperature, $kT/|J|$. The g-factors used to reduce the experimental susceptibilities are those obtained from the least squares refinement discussed earlier. The experimental susceptibilities used for the comparison are smoothed curve values corrected for the temperature independent susceptibility.

For CsCuCl_3 , the magnetic susceptibility parallel to the c-axis is the same as χ_{\parallel} of the Bonner-Fisher model, since the chains are parallel to the c-axis. The magnetic susceptibility

parallel to the a-axis is the same as χ_{\perp} of the Bonner-Fisher model. The comparison between theory and experiment is shown in Figs. 15 and 16. It appears that if the susceptibility is to fit at high temperatures, as it must, it will not fit at low temperatures. The best fit (largest temperature range) seems to be obtained for $J/k = -4^{\circ}\text{K}$. With this value of the exchange integral we can fit our data to the Bonner-Fisher model reasonably well down to approximately 30°K .

This behavior seems to imply that the magnetic interactions in CsCuCl_3 are predominantly one-dimensional in nature down to 30°K whereupon three-dimensional interactions of copper ions on neighboring chains becomes important. Alternatively, it could imply that the Bonner-Fisher model is not valid over a wide temperature range.

Although measurement of the powder magnetic susceptibility showed no indication of three-dimensional ordering, the heat capacity of CsCuCl_3 exhibited a sharp peak at 10.4°K (Rioux and Gerstein, 1969). The heat capacity anomaly had a λ -transition shape consistent with long range ordering. See Fig. 17.

Since reliable estimates for the lattice heat capacity of CsCuCl_3 at low temperatures are not available, it is not possible to determine the magnetic heat capacity in the tempera-

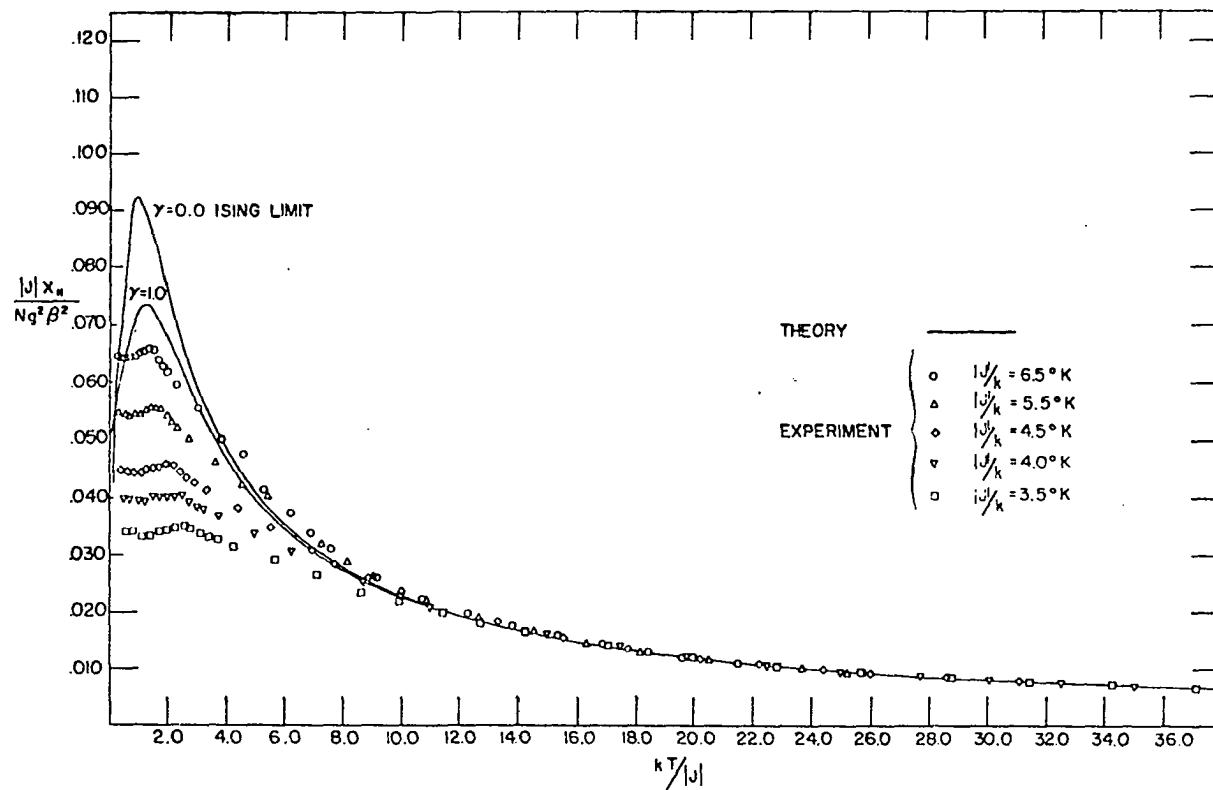


Fig. 15. Comparison of theory and experiment for the parallel magnetic susceptibility. The experimental parallel susceptibilities are the c-axis values

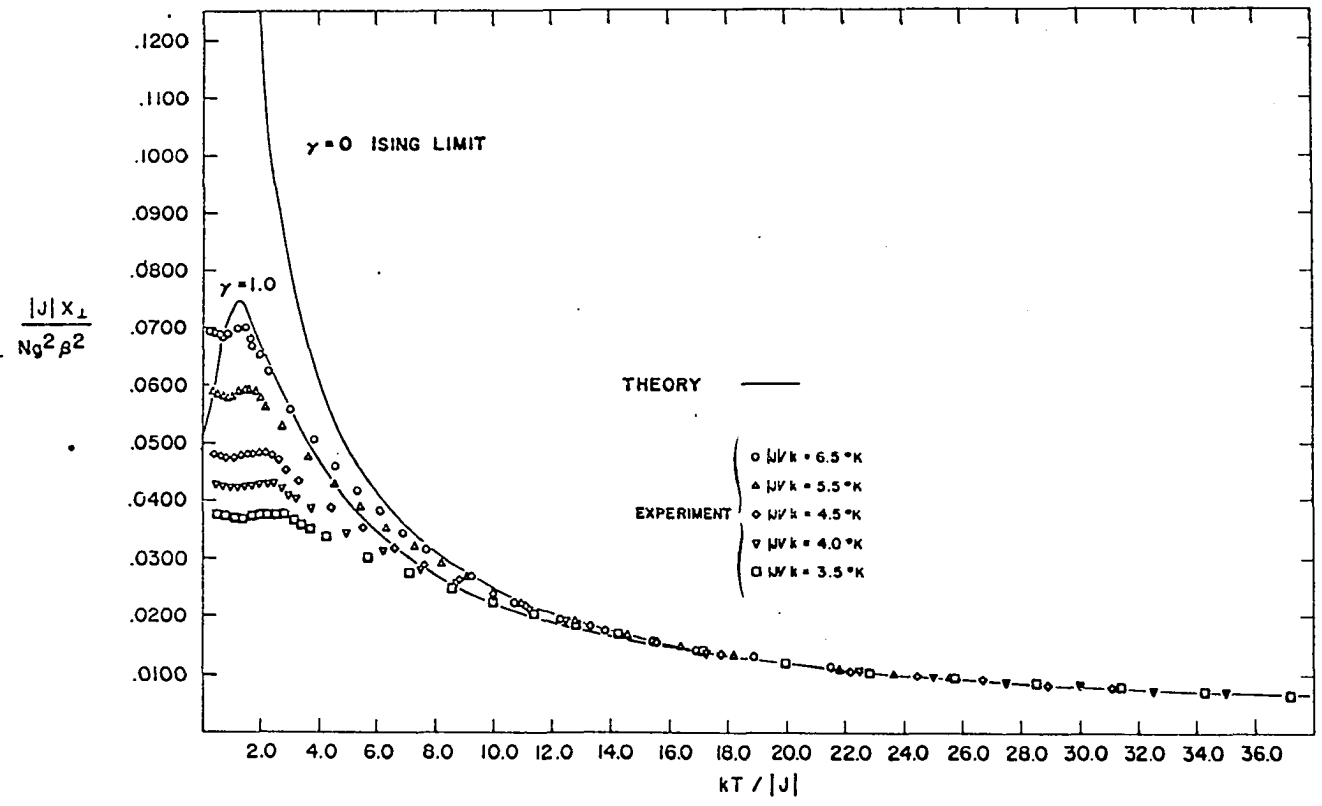


Fig. 16. Comparison of theory and experiment for the perpendicular magnetic susceptibility. The experimental perpendicular susceptibilities are the a-axis values

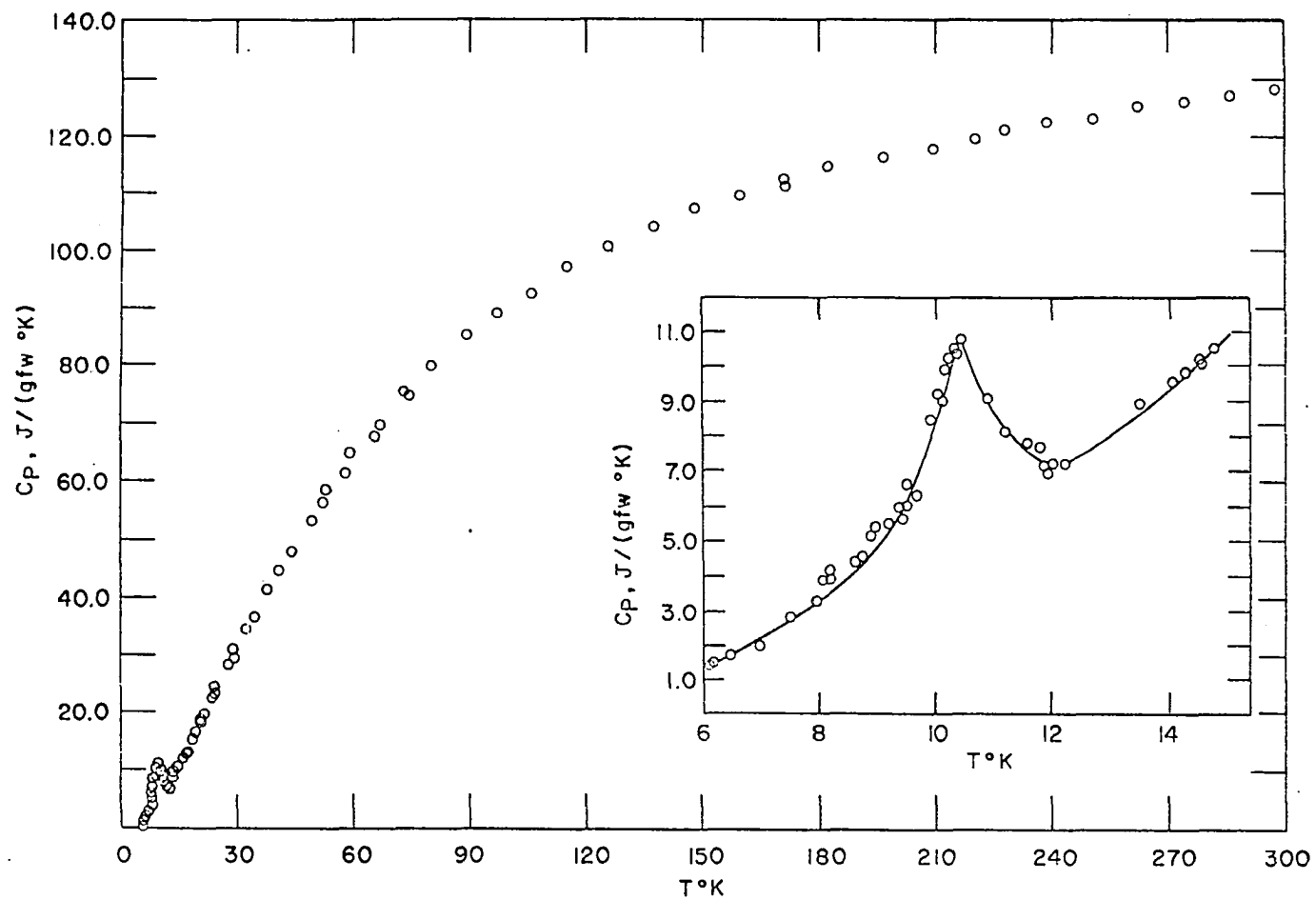


Fig. 17. Heat capacity as a function of temperature for powdered CsCuCl_3 (Rioux and Gerstein, 1969)

ture range 5° to 60°K . Using the magnetic heat capacity, the fraction of the 1.38 e.u. of magnetic entropy lost in long-range ordering could be determined.

We feel that the nature of the heat capacity anomaly is not in disagreement with a model which assumes that the magnetic interactions which become apparent at 55°K are predominantly one-dimensional down to 30°K . At this point the weaker three dimensional interactions become important leading to long range order at approximately 10°K . We observe that whereas the powder magnetic susceptibility exhibited no sharp anomalies in this temperature range, the single crystal magnetic susceptibilities for both a- and c-axis exhibit small cusps at 10°K .

Because the deviation from one-dimensional behavior occurs at such a high temperature it is not possible to determine the extent of the anisotropy of the exchange coupling between spins. To this date one-dimensional systems have either been fit to the completely anisotropic Ising model ($\gamma = 0$) or the completely isotropic Heisenberg model ($\gamma = 0$). No attempts have been made to fit susceptibility data to models of intermediate anisotropy.

The Cu-Cu distance of 3.062 \AA is relatively short and it

is surprising that the exchange interactions in CsCuCl_3 are not stronger. Overlap calculations of Schleuter (Schleuter, Jacobson and Rundle, 1966) rule out any direct Cu-Cu bonding or direct exchange. A suitable super-exchange mechanism, however, would seem to be through the Cu-Cl-Cu symmetric bridges. In these bridges, the Cu-Cl distances are 2.355 \AA and the Cu-Cl-Cu angle is 73.8° . Super-exchange most likely operates through the bridging chlorines via the 3p and 4s chlorine orbitals. Super-exchange via the p orbitals would be ferromagnetic, since the copper orbitals containing the magnetic electrons would overlap orthogonal p-orbitals on the bridging chlorine. Super-exchange via the s-orbitals would be antiferromagnetic since the copper orbitals would overlap the same s-orbital (Owen and Thornley, 1966). The fact that the interactions in CsCuCl_3 are antiferromagnetic indicate that the latter mechanism is most likely. That the chlorine s-orbital is more important in determining the nature of the exchange interaction would appear to be in contradiction with the interpretation of Rinneberg, Haas and Hartmann (1969) who have determined by NMR studies that the magnetic electrons spend only 0.57% of their time in s-orbitals on the bridging chlorine compared to 9% of their time in chlorine p orbitals.

It is interesting that neither χ_a nor χ_c approach zero at low temperatures. In fact χ_a and χ_c appear to remain relatively constant below 10°K . "Conventional" antiferromagnets, such as MnF_2 (Stout and Matarrese, 1953) are characterized by χ_c 's which approach zero and χ_a 's which remain constant below the Neel temperature. This behavior can be explained if one postulates that the spins order antiferromagnetically along the c-axis. With this type of ordering a magnetic field applied along the c-axis can exert no torque on the aligned spins and the magnetization is zero. When the field is applied parallel to the a-axis, which is perpendicular to the direction of alignment, a torque is exerted on the aligned spins. Thus, there is a net magnetization in this direction and the magnetic susceptibility does not go to zero below the ordering temperature (Kittel, 1966, p. 484). Neutron diffraction studies on MnF_2 (Erickson and Shull, 1951) reveal that the spins do align parallel and antiparallel to the c-axis.

The fact that neither χ_a nor χ_c for CsCuCl_3 approach zero below 10°K seems to indicate that the antiferromagnetic alignment of spins is canted with respect to the crystallographic c-axis. This sort of spin alignment would predict non-zero susceptibilities for both the a- and the c-axis below 10°K

since magnetic fields parallel to these axes would exert a torque on the ordered spins.

Canted antiferromagnetism can be caused by large crystal-line field anisotropies. Therefore we would guess that the spins are aligned parallel and antiparallel to the tetragonal axes of the CuCl_4^- complexes, or lie in a spiral arrangement in the plane of the complex.

SUMMARY

The single crystal magnetic susceptibilities of CsCuCl_3 along the crystallographic a- and c-axes have been measured. Plots of $\chi_M T$ vs T for the a- and c-axes indicate that deviations from Curie-Law behavior begin at approximately 55°K , in agreement with previous measurements of magnetic susceptibility on powdered CsCuCl_3 (Rioux and Gerstein, 1969). Least squares refinement of data above 70°K yields g-factors for the a- and c-axes, which when averaged are in agreement with the powder g-factor.

Attempts to determine whether or not a model which assumes that the predominant interacting species in CsCuCl_3 are square planar CuCl_4^{2-} complexes was not entirely successful. However, the disagreement between the model and experiment was not greatly in excess of the estimated experimental error.

It has been suggested that the deviations from Curie-Law behavior which manifest themselves at 55°K are caused by one-dimensional antiferromagnetic interaction between nearest-neighbor copper ions on the infinite chains. Comparison of experimental data with the calculations of Bonner and Fisher (1964) indicate that J/k is -4°K and that the system begins to deviate from one dimensional behavior at approximately 30°K .

An anomaly in the heat capacity and cusps in the single crystal magnetic susceptibilities indicate that the system orders three-dimensionally at approximately 10°K .

It is also suggested that constant values of the a- and c-axes magnetic susceptibilities below 10°K could be explained by assuming a spin alignment which is canted with respect to the c-axis. Given the tetragonal distortion of the CuCl_4^{2-} complexes it is possible that the spins align parallel and antiparallel to the tetragonal axes of the CuCl_4^{2-} complexes or parallel and antiparallel in the square plane of the CuCl_4^{2-} complexes.

BIBLIOGRAPHY

- Abrahams, S. G., and Williams, H. J., 1963, J. Chem. Phys., 39, 2923.
- Adams, R. W., Barraclough, C. G., Martin, R. L., and Winter, G., 1967, Aust. J. Chem., 20, 2351.
- Anderson, R. J., and Giauque, W. F., 1962, J. Chem. Phys., 46, 2413.
- Bacon, G. E., and Curry, N. A., 1962, Proc. Roy. Soc., A266, 95.
- Ballhausen, C. J., 1962, Ligand Field Theory (New York: McGraw-Hill).
- Ballhausen, C. J., and Gray, H. B., 1964, Molecular Orbital Theory (New York: Benjamin).
- Barraclough, C. G., and Ng, C. F., 1964, Trans. Farad. Soc., 60, 836.
- Beavers, C. A., and Lipson, H., 1934, Proc. Roy. Soc. A146, 570.
- Bonner, J. C., 1968, Numerical Studies on the Linear Ising-Heisenberg Model, unpublished Ph.D. Thesis, Library University of London, London, England.
- Bonner, J. C., and Fisher, M. E., 1962, Proc. Phys. Soc., 80, 508.
- Bonner, J. C., and Fisher, M. E., 1964, Phys. Rev., 135, 640.
- Brooks, J. E., and Domb, C., 1951, Proc. Phys. Soc., A207, 343.
- Brush, S. G., 1967, Rev. Mod. Phys., 39, 883.
- Cable, J. W., Wilkinson, M. K., and Wollan, E. O., 1960, Phys. Rev., 118, 950.
- Curie, P., 1895, Ann. chim. et phys. (7) 5, 289.

- Day, P., 1964, Proc. Chem. Soc., Lond., 18.
- DeHaas, W. J., and Gorter, C. J., 1931, Comm. Leiden, 215a, 4.
- Domb, C, 1960, Adv. Phys., 9, 165.
- Dubicki, L., Harris, C. M., Kokot, E., and Martin, R. L., 1966, Inorg. Chem., 5, 93.
- Duffy, W., and Barr, K. P., 1968, Phys. Rev., 165, 647.
- Erickson, R. A., and Shull, C. G., 1951, Phys. Rev., 83, 208.
- Eyring, H., Walter, J., and Kimball, G. E., 1944, Quantum Chemistry (New York: John Wiley and Sons, Inc.)
- Figgis, B. N., and Harris, C. M., 1959, J. Chem. Soc., 855.
- Figgis, B. N., and Martin, R. L., 1966, Inorg. Chem., 5, 100.
- Fisher, M. E., 1960, Proc. Roy. Soc., A256, 502.
- Fisher, M. E., 1963, J. Math. Phys., 4, 124.
- Forstat, H., and McNeely, D. R., 1961, J. Chem. Phys., 35, 1594.
- Fritz, J. J., and Pinch, H. L., 1957, J. Amer. Chem. Soc., 79, 3644.
- Geballe, J. H., and Giauque, W. F., 1952, J. Amer. Chem. Soc., 74, 3513.
- Gerstein, B. C., 1960, Heat Capacity and Magnetic Susceptibility of Thulium Ethylsulphate, unpublished Ph.D. Thesis, Library, Iowa State University of Science and Technology, Ames, Iowa.
- Griffiths, R. B., 1961, unpublished report. AFRCR-1934.
- Griffiths, R. B., 1964, Phys. Rev., 135, 659.
- Handy, L. C., and Gregory, M. W., 1951, J. Chem. Phys., 19, 1314.

- Haseda, T., and Miedema, A. R., 1961, Physica, 27, 1102
- Helmholz, L., 1947, J. Amer. Chem. Soc., 69, 886.
- Henry, N. F. M., and Lonsdale, K., 1965, International Tables for X-ray Crystallography Vol. I (Birmingham, England: The Kynock Press).
- Inoue, M., Emori, S., and Kubo, M., 1968, Inorg. Chem., 7, 1427.
- Inoue, M., Kishita, S., and Kubo, M., 1967, Inorg. Chem., 6, 900.
- Ising, E., 1925, Z. Physik, 31, 253.
- Jarvis, J. A. J., 1962, Acta. Cryst., 15, 964.
- Kato, M., Jonassen, H. B., and Fanning, J. C., 1964, Chem. Revs., 64, 99.
- Kidd, M. R., Sager, R. S., and Watson, W. H., 1967, Inorg. Chem., 6, 946.
- Kittel, C., 1956, Introduction to Solid State Physics (New York: John Wiley and Sons, Inc.)
- Koizumi, H., Osaki, K., and Watanabe, T., 1963, J. Phys. Soc. Japan, 18, 117.
- Maass, G. J., Gerstein, B. C., and Willett, R. D., 1967, J. Chem. Phys., 46, 401.
- Marshall, W., 1958, J. Phys. Chem. Solids, 7, 159.
- Maxwell, E., 1965, Rev. Sci. Instr., 36, 553.
- Mazzi, F., 1955, Acta Cryst., 8, 137.
- Miedema, A. R. van Kempen, H., Haseda, T., and Huiskamp, W. J., 1962, Physica, 28, 119.
- Miller, A. E., and Jelinek, F. J., 1968, Low Temperature Magnetic Behavior of Several Oxides of Gadolinium, unpublished

paper. South Bend, Indiana, Dept. of Metallurgy, University of Notre Dame.

Morrish, A. H., 1965, *The Physical Principles of Magnetism* (New York: John Wiley and Sons, Inc.).

Neel, L., 1932, Ann. phys. (Paris), 17, 64.

Newell, G. F., and Montroll, E. W., 1953, Revs. Mod. Phys., 25, 353.

Orbach, R., 1959, Phys. Rev., 115, 1181.

Owen, J., and Thornley, J. H. M., 1966, Repts. Prog. Physics. II, 29, 675.

Okamura, T., and Date, M., 1954, Phys. Rev., 94, 314.

Perakis, N., Serris, A., and Karantassis, T., 1956, J. Physique Radium, 17, 134.

Poulis, N. J., and Hardeman, G. E. G., 1952, Physica, 18, 201.

Rinneberg, H., Haas, H., and Hartmann, H., 1969, J. Chem. Phys., 50, 3064.

Rioux, F. J., and Gerstein, B. C., 1969, J. Chem. Phys., 50, 758.

Rogers, R. N., and Dempsey, C. W., 1967, Phys. Rev., 162, 333.

Rundle, R. E., 1957, J. Amer. Chem. Soc., 79, 3372.

Sager, R. S., and Watson, W. H., 1968, Inorg. Chem., 7, 2035.

Schleuter, A. W., Jacobson, R. A., and Rundle, R. E., 1966, Inorg. Chem., 5, 277.

Sherwin, C. W., 1959, *Introduction to Quantum Mechanics* (New York: Holt)

Smart, J. S., 1966, *Effective Field Theories of Magnetism* (Philadelphia: Saunders).

- Soos, Z. G., 1965, J. Chem. Phys., 43, 1121
- Soos, Z. G., 1966, Phys. Rev., 149, 330.
- Spence, R. D., and Murty, C. R. K., 1961, Physica, 27, 850.
- Starr, C., Bitter, F., and Kaufmann, R., 1940, Phys. Rev., 58, 977.
- Stout, J. W., and Chisholm, R. C., 1962, J. Chem. Phys., 36, 979.
- Stout, J. W., and Matarrese, L. M., 1953, Rev. Mod. Phys., 25, 338.
- Van Vleck, J. H., 1932, Electric and Magnetic Susceptibilities (London: Oxford University Press).
- Van Vleck, J. H., 1945, Rev. Mod. Phys., 17, 27.
- Vossos, P. H., Jennings, L. D., and Rundle, R. E., 1960, J. Chem. Phys., 32, 1590.
- Vossos, P. H., Fitzwater, D. R., and Rundle, R. E., 1963, Acta. Cryst., 16, 1037.
- Wasson, J. R., Skyr, Chin-I, and Trapp, C., 1968, Inorg. Chem., 7, 469.
- Watanabe, T., and Haseda, T., 1958, J. Chem. Phys., 29, 1429.
- Wells, A. F., 1947a, J. Chem. Soc., 1662.
- Wells, A. F., 1947b, J. Chem. Soc., 1670.
- Willett, R. D., Dwiggin, C., Jr., Kruh, R. F., and Rundle, R. E., 1963, J. Chem. Phys., 38, 2429.
- Wittekoek, S., Poulis, N. J., and Miedema, A. R., 1964, Physica, 30, 1051.

ACKNOWLEDGEMENTS

I wish to express my thanks to Dr. B. C. Gerstein for suggesting this project which I have found very interesting. I also wish to thank him for his guidance during the course of this work and for his interest in my scientific career.

I also wish to acknowledge many fruitful discussions with Mike Habenschuss and Bill Taylor.

I thank Bill Shickell for providing technical assistance when it was needed.

I am grateful to Dr. Jill Bonner Nagle for providing me with a copy of her thesis.

APPENDIX I

Ising Model

The Ising model is characterized by a completely anisotropic coupling between nearest neighbor spins,

$$\mathcal{H} = -2J \sum_{i=1}^N \hat{S}_i^Z \cdot \hat{S}_{i+1}^Z - g\beta H \sum_{i=1}^N \hat{S}_i^Z \quad \text{A-1}$$

With this sort of coupling, although it is somewhat unrealistic physically, it has been possible to obtain an exact, closed expression for the partition function for spin $\frac{1}{2}$ and spin 1 systems. It is therefore possible to calculate exactly all thermodynamic and magnetic properties of an infinite linear chain spin $\frac{1}{2}$ antiferromagnet using the Ising Hamiltonian to describe the interaction between the spins.

The energy eigenvalues of (1) are

$$E(S_1^Z \cdots S_N^Z) = \sum_{i=1}^N \left[-2J(\hat{S}_i^Z \cdot \hat{S}_{i+1}^Z) - g\beta H \hat{S}_i^Z \right] \quad \text{A-2}$$

there being $(2S+1)^N$ such eigenvalues. In this formulation S_i^Z is the eigenvalue of that operator. Therefore, the partition function for a system of N spin $\frac{1}{2}$ atoms is

$$Z(N) = \sum_{S_1^Z} \cdots \sum_{S_N^Z} \exp[-E(S_1^Z \cdots S_N^Z)/kT] \quad \text{A-3}$$

Here the sums are over the spin eigenvalues of the N atoms.

Because of the great simplicity of the spin $\frac{1}{2}$ system the partition function can be written (Stout and Chisholm, 1962; Newell and Montroll, 1953)

$$Z(N) = \text{Trace } P^N \quad \text{A-4}$$

Where,

$$P = \begin{pmatrix} e^{K-B} & e^{-K} \\ e^{-K} & e^{K+B} \end{pmatrix}. \quad \text{A-5}$$

The eigenvalues of the matrix P are

$$\lambda_1 = e^K \cosh B + (e^{2K} \sinh^2 B + e^{-2K})^{\frac{1}{2}} \quad \text{A-6}$$

and

$$\lambda_2 = e^K \cosh B - (e^{2K} \sinh^2 B + e^{-2K})^{\frac{1}{2}}, \quad \text{A-7}$$

where

$$K = J/2kT \quad \text{A-8}$$

and

$$B = g\beta H/kT. \quad \text{A-9}$$

Because the trace (sum of the diagonal elements after the matrix has been diagonalized) is raised to the nth power, only the largest eigenvalue need be considered in the limit of an infinite chain of atoms.

Thus,

$$Z(N) = [e^K \cosh B + (e^{2K} \sinh^2 B + e^{-2K})^{\frac{1}{2}}]^N. \quad \text{A-10}$$

The mathematics can be checked by setting $K = 0$, i.e. no spin-

spin interactions. If this is done

$$Z(N) = (2 \cosh g\beta H/kT)^N \quad \text{A-11}$$

or

$$Z(N) = [\exp(\frac{g\beta H}{2kT}) + \exp(-\frac{g\beta H}{2kT})] \quad \text{A-12}$$

which is the partition function we would write for N spins in the presence of a magnetic field.

With the partition function (A-10) it is then possible to calculate the magnetic susceptibility parallel to the infinite chains using the statistical mechanical expression for χ ,

$$\chi = kT \frac{\partial^2 \ln Z(N)}{\partial H_z^2} \quad \text{A-13}$$

The results of this calculation are,

$$\chi = \frac{Ng^2\beta^2}{4kT} \exp(-J/kT) \quad \text{A-14}$$

Fisher (1963) has calculated the Ising model perpendicular magnetic susceptibility. The results of his calculation are

$$\chi = \frac{Ng^2\beta^2}{4|J|} [\tanh K + K \operatorname{sech}^2 K]. \quad \text{A-15}$$

APPENDIX II

Bonner-Fisher Calculations

Bonner and Fisher (1964) were the first to calculate the thermodynamic properties of rings of spin $\frac{1}{2}$ atoms using the anisotropic Heisenberg Hamiltonian,

$$\mathcal{H} = -2J \sum_{i=1}^N (\hat{S}_i^z \cdot \hat{S}_{i+1}^z + \gamma (\hat{S}_i^x \cdot \hat{S}_{i+1}^x + \hat{S}_i^y \cdot \hat{S}_{i+1}^y)) \quad \text{A-16}$$

They made calculations for $N = 2$ to 11 and $\gamma = 0$ to 1. The results of their calculations show that the thermal and magnetic properties of infinite linear chain systems are well approximated by finite rings of 10 and 11 spins.

Orbach (1959) calculated the energy eigenvalues of the completely isotropic ($\gamma = 1.0$) Heisenberg Hamiltonian for rings of 2, 4, 6, 8 and 10 spins. Griffiths (1964) calculated the thermal and magnetic properties, using the isotropic Heisenberg Hamiltonian, for rings of 2 through 10 spins.

In this section a prototype of the calculation made by Bonner and Fisher will be discussed. The method of calculation is the same as that of Orbach and Griffiths, only the Hamiltonian differs.

Consider a ring of four spins ($n = 4$), i.e.

$$S_{N+1} = S_1 .$$

It is assumed that the Hamiltonian expressing the mutual interactions between these spins is the anisotropic Heisenberg Hamiltonian given by Equation A-16. By making use of stepping operators,

$$\hat{S}^+ = (\hat{S}_x + i\hat{S}_y) \quad \text{A-17}$$

$$\hat{S}^- = (\hat{S}_x - i\hat{S}_y) \quad \text{A-18}$$

it is possible to write the operators S_x and S_y in the following way

$$\hat{S}_x = (\hat{S}^+ + \hat{S}^-)/2 \quad \text{A-19}$$

$$\hat{S}_y = (\hat{S}^+ - \hat{S}^-)/2i. \quad \text{A-20}$$

It is then an easy matter to show that the Hamiltonian (A-16) can be written.

$$\mathcal{H} = -2J \sum_{i+1}^N (\hat{S}_i^z \cdot \hat{S}_{i+1}^z + \frac{1}{2}\gamma(\hat{S}_i^+ \cdot \hat{S}_{i+1}^- + \hat{S}_i^- \cdot \hat{S}_{i+1}^+)) \quad \text{A-21}$$

Now that the Hamiltonian is in a tractable form, it is now necessary to decide how to specify the wavefunctions of the system. Since there are four spins, with each spin having two possible eigenstates $S_z = \pm \frac{1}{2}$, there are 2^4 or 16 possible wavefunctions. Given the form of the M Hamiltonian (A-21) it is best to write the wavefunctions as products of the S_z values of the individual spins. In other words, the wavefunctions will be of the form (++++), (+++-), etc.

In the absence of any interaction between the spins, the 16 wavefunctions are degenerate. Thus, to consider the effect of an interaction of the type (A-21) on a ring of four spins it is necessary to use degenerate perturbation theory. The elements of a 16x16 perturbation matrix must be determined.

These are all possible matrix elements of the perturbing Hamiltonian, H, between all the wavefunctions and have the form (+++-/H/+++), (+++-/H/++++), etc. The Hamiltonian for N = 4 is,

$$\mathcal{H} = -2j(\hat{S}_1^z \hat{S}_2^z + \hat{S}_2^z \hat{S}_3^z + \hat{S}_3^z \hat{S}_4^z + \hat{S}_4^z \hat{S}_1^z) + \frac{1}{2}\gamma(\hat{S}_1^+ \hat{S}_2^- + \hat{S}_1^- \hat{S}_2^+ + \hat{S}_2^+ \hat{S}_3^- + \hat{S}_2^- \hat{S}_3^+ + \hat{S}_3^+ \hat{S}_4^- + \hat{S}_3^- \hat{S}_4^+ + \hat{S}_4^+ \hat{S}_1^- + \hat{S}_4^- \hat{S}_1^+)$$

$$\hat{S}_4^+ \hat{S}_1^- + \hat{S}_4^- \hat{S}_1^+)) .$$

A-22

The perturbation matrix giving the matrix elements between the 16 wavefunctions using this Hamiltonian are given in Table 9.

It is seen that the large matrix "blocks out" along the diagonal into five smaller matrices, two 1x1 matrices, two 4x4 matrices, and a 6x6 matrix. The two 1x1 matrices correspond to total $S_z = \pm 2$, the two 4x4 matrices correspond to total $S_z = \pm 1$, and the 6x6 matrix corresponds to total $S_z = 0$.

Diagonalization of these matrices yields the eigenvalues of the perturbing Hamiltonian plus the zero-order eigenfunctions. The two 1x1 matrices are trivial and have eigenvalues of -2. The 4x4's and the 6x6 were diagonalized by machine using the

Table 9. Perturbation matrix

	(++++)	(+++-)	(+-++)	(+--+)	(-+++)	
(++++)	-2					
(+++-)	0	$-\gamma$	0	$-\gamma$		
(+-++)	$-\gamma$	0	$-\gamma$	0		
(+--+)	0	$-\gamma$	0	$-\gamma$		
(-+++)	$-\gamma$	0	$-\gamma$	0		
	(++--)	(+--+)	(--++)	(-+-)	(+-+-)	(-+-)
(++--)	0	0	0	0	$-\gamma$	$-\gamma$
(+--+)	0	0	0	0	$-\gamma$	$-\gamma$
(--++)	0	0	0	0	$-\gamma$	$-\gamma$
(-+-)	0	0	0	0	$-\gamma$	$-\gamma$
(+-+-)	$-\gamma$	$-\gamma$	$-\gamma$	$-\gamma$	2	0
(-+-)	$-\gamma$	$-\gamma$	$-\gamma$	$-\gamma$	0	2
	(+----)	(-+--)	(--+-)	(----)	(----)	
(+----)	0	$-\gamma$	0	$-\gamma$		
(-+--)	$-\gamma$	0	$-\gamma$	0		
(--+-)	0	$-\gamma$	0	$-\gamma$		
(----)	$-\gamma$	0	$-\gamma$	0		
(----)						-2

subroutine EIGEN.

The eigenvalues and eigenvectors for the calculation with $\gamma = 1.0$ are given in Table 10. The eigenvectors are important in that they can be used to calculate both short- and long-range order which can then be compared with neutron diffraction results. (See Bonner and Fisher, 1964, p. A655). The results of energy eigenvalues calculation as a function of the anisotropic term γ are summarized in Table 11 and Fig. 18.

Now that we have energy eigenvalues it is possible to write a partition function, which means that it is possible to calculate the thermal and magnetic properties of the ring. Since this work is mainly concerned with magnetic properties, the magnetic susceptibility of a ring of 4 spins will be calculated in zero field.

The zero field magnetic susceptibility is calculated using the formula (Ballhausen, 1962),

$$X_i = N \sum_{n,m} \frac{((E_{n,m}^{(1)})^2/kT - 2E_{n,m}^{(2)}) \exp(-E_n^0/kT)}{\sum_n \exp(E_n^0/kT)} \quad A-23$$

where

$$E_{n,m}^{(1)} = (\psi_{n,m}/\mu_i / n,m) = (\psi_{n,m}/\beta(L_i + 2S_i))/\psi_{n,m} \quad A-24$$

where i refers to x-, y- or z-direction and the n and m are quantum numbers labeling the energy levels. If the $\psi_{n,m}$'s are

Table 10. Eigenvalues (in units of $E/|J|$) and eigenvectors for $\gamma = 1.0$ for a ring of four spins

S_z	$E/ J $	Eigenfunctions
+2	+2	$\psi_1 = 1.000 ++++\rangle$
+1	+2	$\psi_2 = 0.500 +++-\rangle + 0.500 ++-+\rangle + 0.500 +-++\rangle + 0.500 -+++ \rangle$
+1	0	$\psi_3 = -0.185 \quad -0.683 \quad +0.185 \quad +0.683$
+1	0	$\psi_4 = -0.683 \quad +0.185 \quad +0.683 \quad -0.185$
+1	-2	$\psi_5 = 0.500 \quad -0.500 \quad +0.500 \quad -0.500$
-1	+2	$\psi_6 = 0.500 +---\rangle + 0.500 -+--\rangle + 0.500 --+-\rangle + 0.500 ---+ \rangle$
-1	0	$\psi_7 = -0.185 \quad -0.683 \quad +0.185 \quad +0.683$
-1	0	$\psi_8 = -0.683 \quad +0.185 \quad +0.683 \quad -0.185$
-1	-2	$\psi_9 = 0.500 \quad -0.500 \quad +0.500 \quad -0.500$
0	+2	$\psi_{10} = 0.408 ++--\rangle + 0.408 +- -+\rangle + 0.408 --++\rangle + 0.408 -++-\rangle + 0.408 +-+-\rangle + 0.408 -+-+\rangle$
0	0	$\psi_{11} = -0.318 \quad -0.280 \quad -0.268 \quad +0.8654 \quad +0.000 \quad +.000$
0	0	$\psi_{12} = -0.426 \quad -0.375 \quad +0.823 \quad -0.028 \quad +0.000 \quad +0.000$
0	0	$\psi_{13} = -0.684 \quad +0.729 \quad -0.023 \quad -0.023 \quad +0.000 \quad +0.000$
0	-2	$\psi_{14} = 0.000 \quad +0.000 \quad 0.000 \quad 0.000 \quad -0.707 \quad +0.707$
0	-4	$\psi_{15} = -0.289 \quad -0.2887 \quad -0.289 \quad -0.289 \quad +0.577 \quad +0.577$
-2	+2	$\psi_{16} = 1.000 ----\rangle$

Table 11. Energies in units of $E/|J|$ as a function of γ and S_z

S_z	Number of states	$\gamma=.1$	$\gamma=.2$	$\gamma=.3$	$\gamma=.4$	$\gamma=.5$	$\gamma=.6$	$\gamma=.7$	$\gamma=.8$	$\gamma=.9$	$\gamma=1.0$
± 2	2	2.00	2.00	2.00	2.00	2.00	2.00	2.00	2.00	2.00	2.00
± 1	2	0.20	0.40	0.60	0.80	1.00	1.20	1.40	1.60	.80	2.00
	4	0.00	0.00	0.00	0.00	0.00	0.00	0.00	0.00	.00	0.00
	2	-0.20	-0.40	-0.60	-0.80	-1.00	-1.20	-1.40	-1.60	-1.80	-2.00
0	1	+0.039	.1487	.3115	.5100	.732	.970	1.22	1.474	1.735	2.00
	3	0.00	0.00	0.00	0.00	0.00	0.00	0.00	0.00	0.00	0.00
	1	-2.04	-2.15	-2.31	-2.51	-2.73	-2.97	-3.22	-3.474	-3.735	-4.00
	1	-2.00	-2.00	-2.00	-2.00	-2.00	-2.00	-2.00	-2.00	-2.00	-2.00

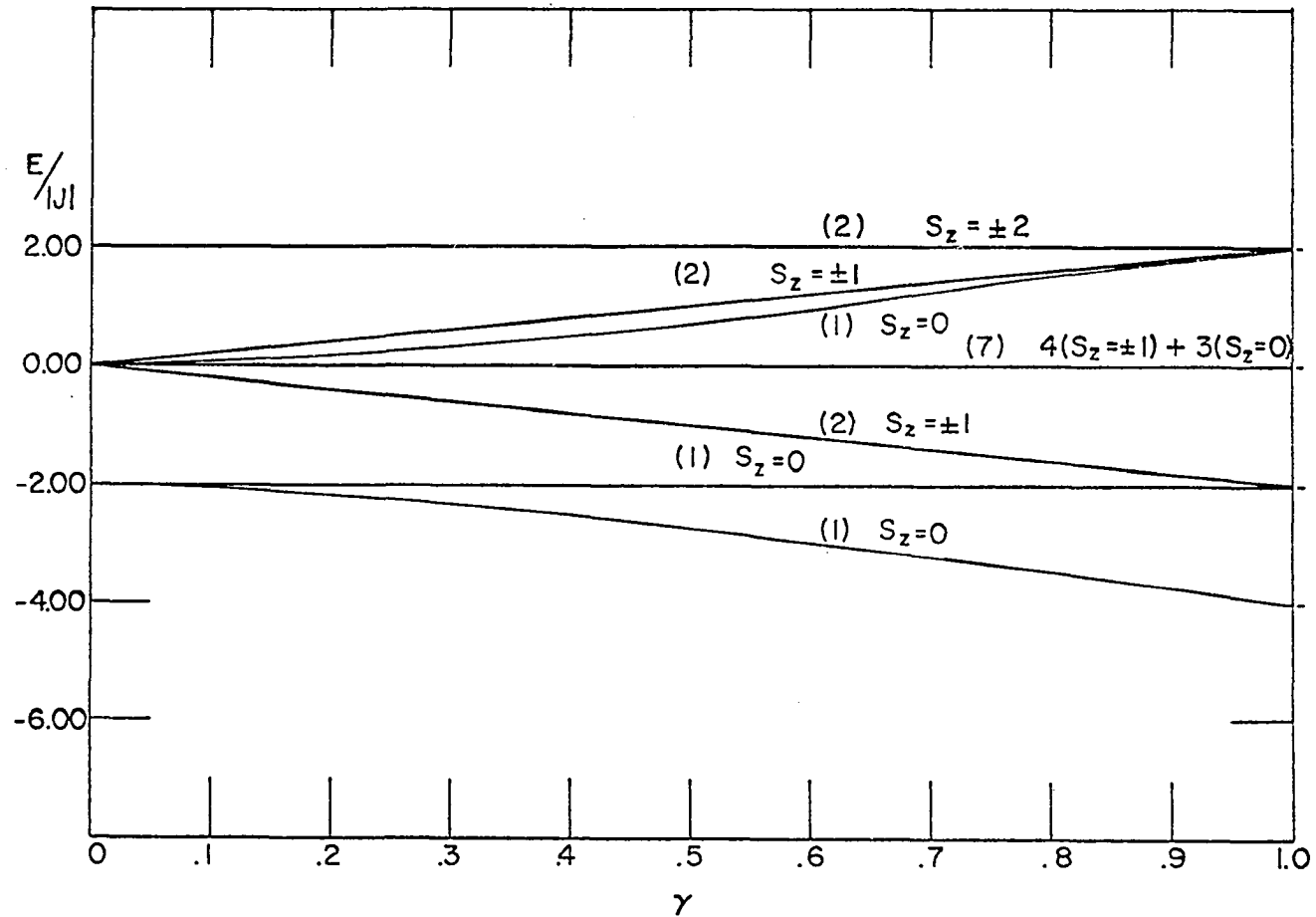


Fig. 18. Energy eigenvalues (in units of $E/|J|$) as a function of γ for a ring of four spins

degenerate, degenerate perturbation theory must be used to calculate $E_{n,m}^{(1)}$. For example we consider the z-direction and neglect the orbital contribution to the magnetic moment and the temperature independent term.

$$\chi = \frac{Ng^2\beta^2}{kT} \frac{(2e^{2J/kT} + 4e^{0J/kT} + 10e^{-2J/kT})}{(e^{4J/kT} + 3e^{2J/kT} + 7e^{0J/kT} + 5e^{-2J/kT})}. \quad \text{A-25}$$

The results of these calculations are summarized in Fig. 19.

In summary, Bonner and Fisher have made calculations of the type described above for $N = 2, 11$. After determining the eigenvalues and eigenvectors for the various rings, they wrote a partition function and calculated the thermodynamic functions $E - E_0$ and S , and the magnetic susceptibility $J \chi / Ng^2\beta^2$. These results may be checked experimentally by the measurement of the heat capacity and the single crystal magnetic susceptibility.

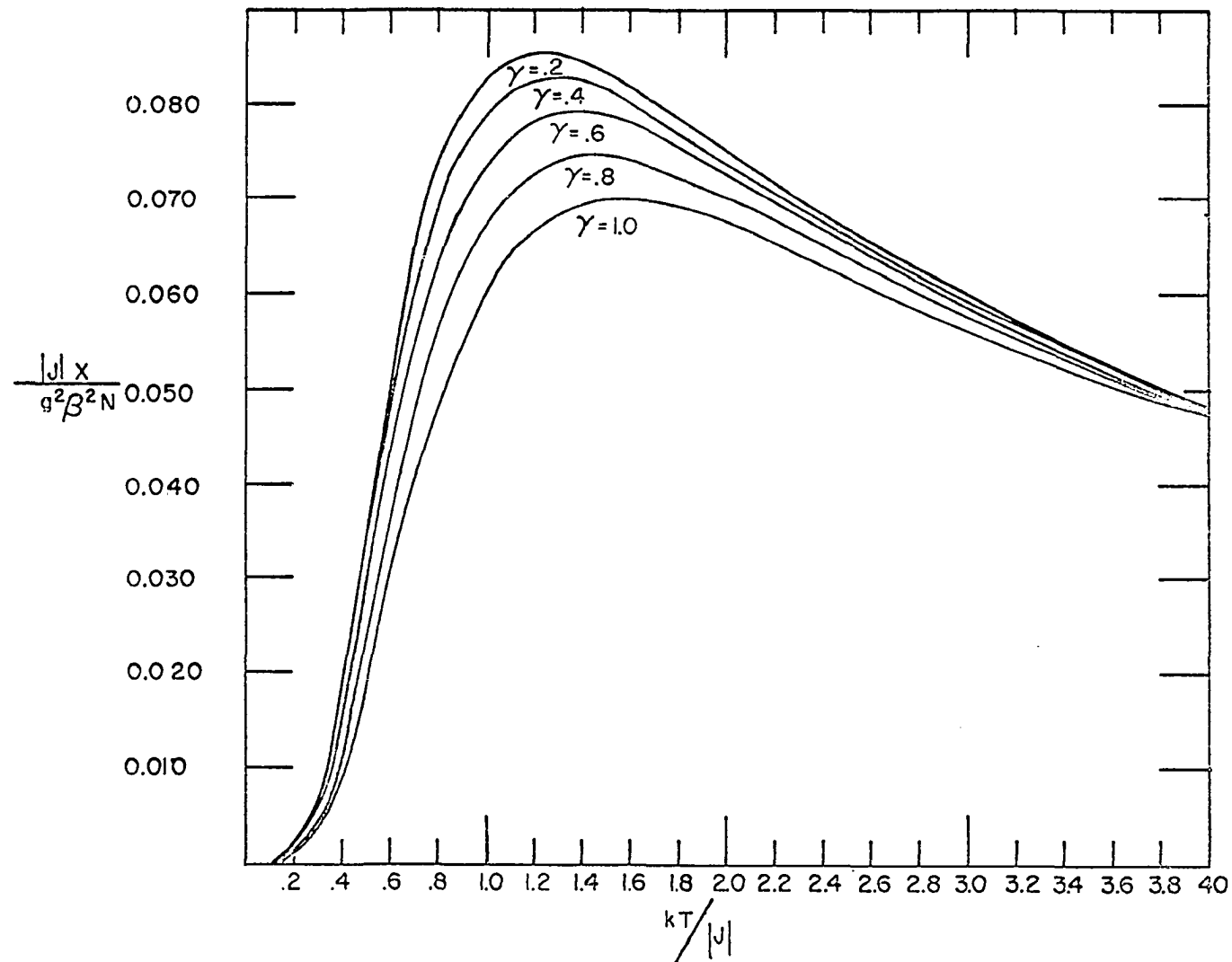


Fig. 19. Magnetic susceptibility as a function of reduced temperature for a ring of four spins for selected values of γ

APPENDIX III

Molecular Orbitals for CuCl_4^-

The following molecular orbitals are based on the coordinate system shown in Fig. 20.

$$B_{1g}(\sigma^*): \quad |\emptyset_{x^2-y^2}\rangle = \alpha |dx^2-y^2\rangle - (1-\alpha^2)^{\frac{1}{2}} \frac{1}{2} [-|p,x,1\rangle \\ + |p,y,2\rangle + |p,x,3\rangle - |p,y,4\rangle]$$

$$B_{2g}(\pi^*): \quad |\emptyset_{xy}\rangle = \gamma |dxy\rangle - (1-\gamma^2)^{\frac{1}{2}} \frac{1}{2} [|p,y,1\rangle \\ + |p,x,2\rangle - |p,y,3\rangle - |p,x,4\rangle]$$

A-26

$$E_g(\pi^*): \quad |\emptyset_{yz}\rangle = \gamma |dyz\rangle - (1-\gamma^2)^{\frac{1}{2}} \frac{1}{2} [|p,z,2\rangle - |p,z,4\rangle] \\ |\emptyset_{xz}\rangle = \gamma |dyz\rangle - (1-\gamma^2)^{\frac{1}{2}} \frac{1}{2} [|p,z,1\rangle - |p,z,3\rangle]$$

$$A_{1g}(\sigma^*): \quad |\emptyset_z^2\rangle = \alpha |dz^2\rangle - (1-\alpha^2)^{\frac{1}{2}} \frac{1}{2} [|p,x,1\rangle \\ + |p,y,2\rangle - |p,x,3\rangle - |p,y,4\rangle]$$

The notation $|p,x,2\rangle$ refers to the P_x orbital on chlorine 2, using the coordinate system of Fig. 20.

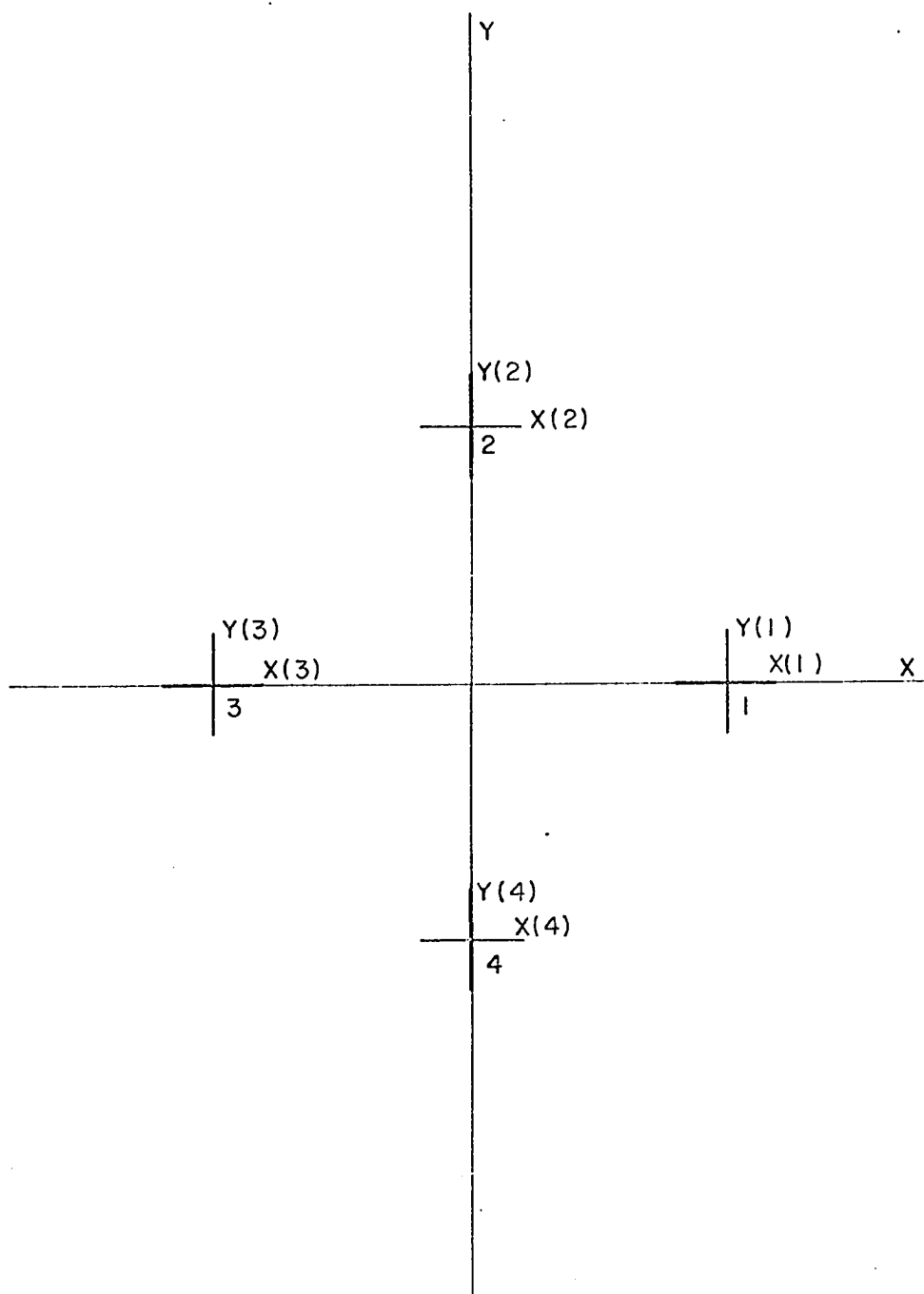


Fig. 20. Coordinate system for CuCl_4^{2-} complexes